รายงานวิจัยฉบับสมบูรณ์

โครงการพัฒนาการใช้เซลล์ต้นกำเนิดชนิดเมสเซนไคน์มอลจากเนื้อเยื่อไขมันชั้นใต้ผิวหนังและไขมันใต้เข่าในการสร้างเนื้อเยื่อกระดูกอ่อน

โดย นพ.ดร.ตุลยพฤกษ์ ถาวรสวัสดิ์รักษ์

เมษายน 2561

สัญญาเลขที่ MRG5480107

รายงานวิจัยฉบับสมบูรณ์

โครงการพัฒนาการใช้เซลล์ต้นกำเนิดชนิดเมสเซนไคน์มอล จากเนื้อเยื่อไขมันชั้นใต้ผิวหนังและไขมันใต้เข่าในการสร้างเนื้อเยื่อกระดูกอ่อน

นพ.ดร.ตุลยพฤกษ์ ถาวรสวัสดิ์รักษ์
คณะแพทยศาสตร์โรงพยาบาลรามาธิบดี มหิดล

สนับสนุนโดยสำนักงานกองทุนสนับสนุนการวิจัย

รูปแบบ Abstract (บทคัดย่อ)

Project Code : MRG5480107

Project Title : โครงการพัฒนาการใช้เซลล์ต้นกำเนิดชนิดเมสเซนไคน์มอลจากเนื้อเยื่อไขมันชั้นใต้ผิวหนังและไขมันใต้เข่าในการสร้างเนื้อเยื่อกระดูกอ่อน (Establishing adipose derived mesenchymal stem cell based approach from subcutaneous and infrapatellar knee fat for cartilage regeneration)

Investigator : นพ.ดร.ตุลยพฤกษ์ ถาวรสวัสดิ์รักษ์ คณะแพทยศาสตร์โรงพยาบาลรามาธิบดี มหิดล

E-mail Address : Tulyapruek@gmail.com

Project Period : 2 พฤษภาคม 2559 ถึง 2 พฤษภาคม 2561

Abstract

Once damaged, the articular cartilage has very limited intrinsic capacity for self-renewal due to its avascular nature. As a result, damaged cartilage often leads to pain if left untreated, and gradually develop OA overtime. Stem cell based approach have been focused on repairing damaged cartilage in the patient with early stage of OA. However, there are no effective source for mesenchymal stem cells (MSCs) to repair the defect. In the recent study adipose-derived mesenchymal stem cells (ASCs) have been demonstrated to be superior to Bone marrow derived MSCs (BM-MSCs) for the cartilage regeneration. Therefore, the present study aimed to establish the potential of using scaffold free cartilage construct derived from ASCs as a new therapy for cartilage regeneration in a rat model of osteochondral defect. The in vitro characteristics between ASCs from infrapatellar fat pad and subcutaneous tissue were evaluated. There was no difference in the number of CFUs and size of CFUs between IPFP and SC sources. ASCs isolated from both sources had a normal karyotype. The mesenchymal stem cells (MSCs) markers on flow cytometry was equivalent. IPFP-ASCs demonstrated significantly higher expression of SOX-9 and RUNX-2 over ASCs isolated from SC (6.19 ± 5.56-, 0.47 ± 0.62-fold; p value = 0.047, and 17.33 ± 10.80-, 1.56 ± 1.31-fold; p value = 0.030, resp.). The one of the TGF-b signal pathway of ASCs infrapatellar knee namely GDF-5 has been evaluated from the patients with OA in the different severities (KL 3

and KL 4). GDF-5 expression from synovial tissue is correlated with the severity according to KL score. Moreover, the TGF-b signal pathway including pathway activity signature genes, TGF beta superfamily Ligans, TGF beta Superfamily receptors, Transcription factors and regulators as well as SMAD Target genes were significantly higher expression in IPFP-ASCs. However, in the preclinical study using osteochondral model for cartilage construct implantation, there was no statistically difference in macroscopic observations and histological examination of IF-ASCs and SC-ASCs at 4 weeks post-implantation. The quantitative measurement of immunostaining for type II collagen and aggrecan also revealed that no significant differences were also observed between these constructs. In this study, the infrapatellar fat pad tissue could serve as the potential source for cartilage repair. It is suggested that implantation of scaffold free cartilage construct derived from IF-ASCs may be served as an alternative approach to repair the cartilage defect. However, further studies are required to confirm this finding.

บทคัดย่อ

เนื่องจากกระดูกอ่อนที่บริเวณผิวข้อไม่มีเลือดมาเลี้ยง ทำให้เมื่อเกิดการบาดเจ็บ จะไม่สามารถฟื้นฟูตัวเองได้ ดังนั้นจะส่งผลให้เกิดความเจ็บปวดและถ้าการบาดเจ็บนี้ไม่ได้รับการรักษาอาจจะเป็นสาเหตุทำให้เกิดโรคข้อเข่าเสื่อมได้ในเวลาต่อมา ปัจจุบันนี้ได้มีความพยายามในการนำเซลล์ต้นกำเนิดจากไขกระดูกมาใช้ในการรักษาผู้ป่วยที่เป็นโรคข้อเข่าเสื่อมในระยะแรก แต่มีรายงานพบว่าเซลล์ต้นกำเนิดจากเนื้อเยื่อไขมันนั้นมีประสิทธิภาพที่ดีกว่าเซลล์ต้นกำเนิดจากไขกระดูกในการฟื้นฟูกระดูกอ่อนที่บริเวณผิวข้อ ประกอบกับมีงานวิจัยส่วนน้อยที่ทำการศึกษาความสัมพันธ์ระหว่างการเปลี่ยนแปลงสภาพเนื้อเยื่อกับการเกิดความเจ็บปวด ด้วยเหตุนี้ในงานวิจัยนี้ จึงมีวัตถุประสงค์ในการศึกษา ความสามารถในการฟื้นฟูกระดูกอ่อนผิวข้อและเซลล์ต้นกำเนิดชนิดมีเซนไคมอลจากเนื้อเยื่อไขมันที่ผิวหนัง และเนื้อเยื่อไขมันใต้เข่าโดยไม่ใช้วัสดุที่เป็นโครงร่าง โดยลักษณะของเซลล์ที่ได้จากแหล่งทั้งสองมีคุณสมบัติใกล้เคียงกัน แต่เซลล์ต้นกำเนิดชนิดมีเซนไคมอลจากเนื้อเยื่อไขมันใต้เข่าสามารถถูกเหนี่ยวนำไปเป็นกระดูกอ่อนได้ดีกว่า และ ยีนในกลุ่ม TGF-b signal pathway ซึ่งประกอบด้วย pathway activity signature genes, TGF beta superfamily Ligans, TGF beta Superfamily receptors, Transcription factors and regulators และ SMAD Target genes อาจจะเกี่ยวข้องกับคุณสมบัติที่ถูกเหนี่ยวนำของเซลล์ นอกจากนั้นได้ทำการทดลองกับหนูที่ถูกชักนำให้เกิดการบาดเจ็บที่กระดูกอ่อนผิวข้อ จากผลการทดลองพบว่าเมื่อฝังเซลล์ต้นกำเนิดชนิดมีเซนไคมอลที่ได้จากเนื้อเยื่อไขมันบริเวณสะบ้าหัวเข่าเข้าไปที่เข่าของหนู สามารถจะฟื้นฟูให้กระดูกอ่อนผิวข้อชนิดไฮยาลีนเจริญได้ และยังคงมีประสิทธิภาพในการสร้างกระดูกอ่อนเป็นระยะเวลาถึง 4 สัปดาห์ ได้ใกล้เคียงกันกับในเซลล์ต้นกำเนิดชนิดมีเซนไคมอลจากเนื้อเยื่อไขมันที่ผิวหนัง และเนื้อเยื่อไขมันใต้เข่า เซลล์ต้นกำเนิดชนิดมีเซนไคมอลจากเนื้อเยื่อไขมันบริเวณสะบ้าหัวเข่าสามารถ

นำมาใช้เป็นทางเลือกใหม่ในการรักษาการบาดเจ็บของกระดูกอ่อนผิวข้อ อย่างไรก็ตาม ควรมีการศึกษาเพิ่มเติมเพื่อยืนยันการค้นพบที่เกิดขึ้น

Keywords : osteoarthritis, mesenchymal stem cells, articular cartilage, osteochondral defect

คำสำคัญ: โรคข้อเสื่อม, เซลล์ต้นกำเนิดชนิดเมสเซนไคน์มอล, กระดูกอ่อนผิวข้อ, กระดูกอ่อนบาดเจ็บ

Objectives:

(1) To characterize adipose derived MSCs from subcutaneous and infrapatellar knee fat sources

(2) To determine and compare in vitro potential of chondrogenic differentiation from subcutaneous and infrapatellar knee fat source

(3) To evaluation differentiation TGF-b signal pathway of ASCs from subcutaneous and infrapatellar knee during chondrogenic differentiation

(4) To determine and compare chondrogenic regeneration potential of ASCs from subcutaneous and infrapatellar knee fat source in cartilage injury model in rodent

Materials and Methods:

Experimental I: To establish ASCs bank and compare the characteristic of ASCs from subcutaneous and infrapatellar knee fat source

a) Preparation of adiposed-derived mesenchymal stem cell (ASCs)

ASCs will be harvested from two different sources, including infrapatellar fatpad tissue and subcutaneous adipose tissue. Infrapatellar fatpads will be collected from patients who are assigned for total knee arthroplasty. For another group, subcutaneous adipose tissues will be collected from patients who are planning for cosmetic surgery by using lipoaspiration. After harvesting, AT-MSCs will be isolated and culture in Ramathibodi hospital's research center until 3^{rd} passage.

Total 20 participants in either undergoing TKA or undergoing cosmetic liposuction will be included in this study. Patient's age/ Sex/ BMI will be recorded. Radiographic parameter by KL classification also determined.

b) ASCs characterization

ASCs will then be evaluated for immunophenotypes (CD73, CD90, CD105, CD 34, CD45 and HLA-DR) by using flow cytometry. In addition, ASCs' karyotype, bacterial contamination, colony-forming units (CFUs), differentiation abilities to chondrogenic-, adipogenic- and osteogenic-ASCs will also be determined.

Experimental II: To confirm and compare the differentiation of chondrocytes by determining the expression of chondrogenic related genes of ASCs from subcutaneous and infrapatellar knee sources

a) Confirmation of chondrogenic differentiation

To demonstrate the chondrogenic differentiation potential of MSCs, passage 3-4 MSCs were cultured *in vitro* under chondrogenic conditions. to induce chondrogenesis using the micromass culture technique, 4×10^5 cells were resuspended in polypropylene tubes, centrifuged gently to form a micromass, then cultured in serum-free medium containing high-glucose DMEM supplemented with 100 nM dexamethasone, 1x Insulin-transferrin-selenium plus premix (ITS Premix, from BD®); final concentration: 6.25 μ g/mL bovine insulin, 6.25 μ g/mL transferrin, 6.25 μ g/mLselenous acid, 5.33 μ g/mL linoleic acid and 1.25 μ g/mL bovine serum albumin), 50 μ g/mL ascorbic acid, 100 μ g/mL sodium pyruvate, 50 μ g/mL proline, and 20 ng/mL transforming growth factor-b3 (TGF-b3). The medium was changed every 3 days. After 3 weeks, cultured pellets were frozen, sectioned (6 μ m thick), and stained with Alcian blue.

c) Determination of SOX-9 expression

Expression of SOX-9 gene will be quantified using quantitative real-time RT-PCR. Comparative gene expression will be used for quantification. RNA extraction will be performed using tissue RNA extraction kit (Zymo Research, Irvine, California, USA). RNA will be converted to cDNA using SuperScript® VILO™ cDNA Synthesis Kit (Gibco, Life technology, Grand Island, NY, USA). KAPA SYBR®Fast qPCR Master Mix (2x) Universal (KAPA Biosystem, Woburn, MA USA) will be used. Rotorgene 6000 (Qiagen, Hilden, Germany) real-time PCR platform will be used.

d) Confirmation of immunohistology

Cell pellet s were processed by standard histological procedures. They were then stained with Hematoxylin and Eosin (H&E) to detect general morphology. In addition, immunohistochemical staining for aggrecan and type-II collagen were also assessed by using standard immunochemistry techniques.

Experimental III: To evaluation differentiation TGF-b signal pathway of ASCs from subcutaneous and infrapatellar knee during chondrogenic differentiation

a) Sample preparation

For the PCR array, RNA samples were collected and quantified as detailed in the experiment II. To obtain the best results from the PCR array, all RNA samples were selected by the following criteria: i) A260:A230 ratio should be greaterthan 1.7, ii) A260:A280 ratio should be 1.8 to 2.0, iii) concentration determination byA260 should be greater than 40 μ g/ml total RNA; iv) No RNA degradation (checked by ribosomal RNA band integrity). RNA 1.5 μ g from each sample was used to make cDNA using a RT2 First Strand Kit (SABiosciences, Qiagen, Crawley, Sussex, UK). RNA samples were first mixed with 2 μ l GE (5 x gDNA Elimination Buffer) andnuclease-free H2O added up to 10 μ l. The mix was incubated at 42oC for 5 min and chilled on ice immediately for at least 1 min. Then, 10 μ l RT cocktail that included 4 μ l BC3 (5 X RT Buffer3), 1 μ l P2 (Primer & External Control Mix), 2 μ l RE3 (RT Enzyme Mix 3), and 3 μ l Nuclease free water; was added to each 10 μ l RNA mixture. The synthetic reaction mixture was incubated at 42oC for exactly 15 min, and there action was immediately stopped by heating at 95oC for 5 min. Finally, 91 μ l ofnuclease-free H2O was added to each 20 μ l of reaction mixture. The cDNA wasstored at -20oC for later use. For RT2 ProfilerTM PCR Array (PAHS-035A: Human TGF-b BMP Signaling Pathway) The PCR array was conducted using the RT2 PCR Array. The experimental cocktail was prepared as follows: 1350 μ l 2X SABiosciences RT2 qPCR master mix, 102 μ l diluted first strand cDNA synthesis reaction, and 1248 μ l nuclease-free water. This experimental cocktail (25 μ l) was added to each well.iii) For PCR arrays, a two-step cycling program was used on the Bio-Rad by detecting the fluorescent signal released from SYBR-green. Data from each PCR array were input into the respective Excel-

based RT2 RNA QCPCR Array Data Analysis template or RT² Profiler PCR Array Data Analysis Template v3.3 (http://www.sabiosciences.com/pcrarraydataanalysis.php).

This array will screen for expressed genes in TGF-b BMP Signaling Pathway. Growth and differentiation factor is main interesting molecule as it is involved in chodrogenic differentiation.

Experimental IV: ***To compare the alternative source of ASCs from infrapattellar fatpad (IF) and subcutaneous tissue (SC) in a rat model of cartilage defect***

The present study is designed to further investigate whether culture of cartilage progenitor cells derived from either IF-ASCs or SC-ASCs could retain their characteristics and differentiation abilities after implantation in a rat model of cartilage defect in a similar manner to that observed in our preliminary *in vitro* study, in which IF-ASCs are found to exhibit a superior chondrogenic and osteogenic differentiation than that of SC-ASCs. To investigate this, the 3D culture of cartilage constructs derived from either IF-ASCs or SC-ASCs will be implanted into the full-thickness osteochondral defects of the rats and the chondrogenic differentiation markers will be examined by using histological and immunochemistry analyses, in which hyaline cartilage is stained for safranin-O and immunostained for type II collagen.

a) Preparation of three-dimension (3D) cartilage constructs

ASCs will be induced into in the conical tube for 3D culture technique for 21 days using micro-mass technique. Cell staining with Alcian-blue staining will be applied to the chondrocyte differentiation.

b) Animal experimentation

Six weeks old male (160-180 g) wistar rats will be allowed to acclimatize to the new environment for a week and then they will be randomly divided into two main groups that are differed in the duration of convalescence following implantation with cartilage constructs as shown below.

Group A (n=6): Implantation with cartilage construct-derived from IF on one side of femoral condyle and with cartilage-derived construct from SC on the other side of femoral condyle for 4 weeks

Group B (n=6): Implantation with cartilage construct-derived from IF on one side of femoral condyle and with cartilage-derived construct from SC on the other side of femoral condyle for 12 weeks

c) Induction of cartilage defect

After the rats anesthetized, a medial parapatellar incision will be made on the right knee joint of the animal. The patellar will be dislocated laterally to expose a better access to the articular surface of the femoral condyle. Two full-thickness osteochondral defects with a diameter of 1.2 mm will be

created by using Kirschner wires (K-wires) to drill on both medial and lateral femoral condyles until reaching the bone marrow region. The cartilage constructs-derived from either IF or SC will be randomly implanted into either the lateral or medial femoral condyle. The joint capsule and skin will be closed with vicryl 4-0 braided absorbable suture and monofilament 3-0 Nylon threads, respectively. After recovery from surgery, all rats will be returned to cages in groups of two, with free access to food and water.

d) Necropsy (Gross examination of rat knee joint):

At the end of each post implantation time points, animals will be euthanized and a gross necropsy will be performed to assess the knee joint regeneration. Photographs will be taken of each joint at the surgical site. Then knee joint tissues from both hind limbs will be collected for further histological and immunohistochemistry analysis.

e) Histological and immunohistochemistry analyses

In brief, tibiofemoral joints from both knees of each animal will be dissected by cutting mid-femur and tibia and submerged in 10% buffered formalin for 72 h and decalcified with 10% EDTA for 3 weeks, and embedded in paraffin. Sectioning (4 μm sections) will then conducted using standard microtome and will be stained with hematoxylin and eosin (H & E) and safranin-O. Histopathological analysis will be assessed in a semiquantitative blinded fashion and scored according to the scoring system.

For the immunostaining of type II collagen, the joint tissues will be processed by standard immunochemistry techniques. In brief, sections will be deparaffinized and the endogenous peroxidase activity will be blocked with 0.5% hydrogen peroxide in methanol and washed in 0.1% bovine serum albumin (BSA) in Tris-buffered saline (TBS). The sections will be treated with testicular hyaluronidase, in which a non-specific staining will be reduced by incubation with horse serum. The sections will then be incubated with monoclonal antibody against human type II collagen and the immunostaining will be performed using the Vectastain avidin-biotin peroxidase complex (ABC) kit (Vector Laboratories, Burlingame, CA, USA).

Results:

(1) Characterization of IMSCs and SMSCs (objective 1 and 2)

Abbreviations

IMSCs = Infrapatellar fatpad mesenchymal stem cells

SMSCs = Subcutaneous mesenchymal stem ceslls

Demographic data

In this study, 5 female participants were underwent total knee arthroplasty operation. Infrapatellar fatpad tissue was collected by sterile technique then ASCs was extracted. Range of patient' age was from 53-77 years and range of BMI was from 20.24-26.53 kg/m^2. All participants were diagnosed OA Right knee stage 4 by KL classification. The infrapatellar fat tissue was measured for weight range from 8.63-14.75 gram and for yield for cell extraction, range from $7.88x10^6$-$67.79x10^6$ cell/ml/gram. Timing for cell culture from passage 0^{th} to passage 2^{nd} was about 15-28 days and number of ASCS in passage 2^{nd} was counted by hemocytometer and range from $0.30x10^6$–$3.37x10^6$ cell/ml (Table 1).

Table 1: Baseline characteristics of ASCs from infrapatellar fatpad

	Case 1	Case 2	Case 3	Case 4	Case 5
Sex	Female	Female	Female	Female	Female
Age (yrs)	77	53	71	66	62
BMI (kg/m^2)	26.53	27.01	24.44	20.50	20.24
Side of TKA operation	Right	Right	Right	Right	Right
OA classification	Stage 4	Stage 4	Stage 4	Stage 4	Stage 4
Fatpad weight (gram)	13.49	13.49	10.25	8.63	14.75
Number of ASCs isolation(P 0*) ($x10^6$cells/ml)	9.10	1.25	6.95	1.43	1.16
Yield of ASCs Collection(P 0*) ($x10^4$cells/ml/gram)	67.46	9.27	67.79	16.51	7.88
Incubation time to P2** (days)	17	28	17	17	15
Number of ASCs at P2**($x10^6$cells/ml)	3.30	3.37	2.26	0.30	2.30

* Passage 0^{th}

** Passage 2^{nd}

In evaluation ASC's properties in other source (subcutaneous tissue, N=5), we found non-statistical significant in gender and BMI of participants both group (p-value=1.000 and p-value=0.001, respectively) but the mean age in subcutaneous group was lower than infrapatellar fat pad group (p-value=0.001). Weight of adipose tissue from lipoaspiration was more than TKA operation (49.75±20.57, 12.12±2.57; p-value=0.014). Number of ASCs isolation after sample collection was counted by hemocytometer and found non-statistical significantly in both groups (p-value=0.923) but infrapatellar fatpad group had yield of ASCs collection more other group (33.78±31.07 and 9.28±7.23, respectively; p-value=0.076). ASCS was cultured in T25 plate though to passage 2nd about 18.80±5.22 and 23.00±7.52 days, respectively (p-value=0.341) and the number of ASCs was found non-statistical significant in ASCs number in both groups (p-value=0.877), as shown in table 1

ASCs immunophenotypes

We found non-statistical significantly of ASCs' phenotype from flow cytometry in both groups. Positive markers for MSCs were shown by CD73, CD 90 and CD105. Negative markers for MSCs were shown by CD 34, CD 45 and HLA-DR (Table 2, figure 1)

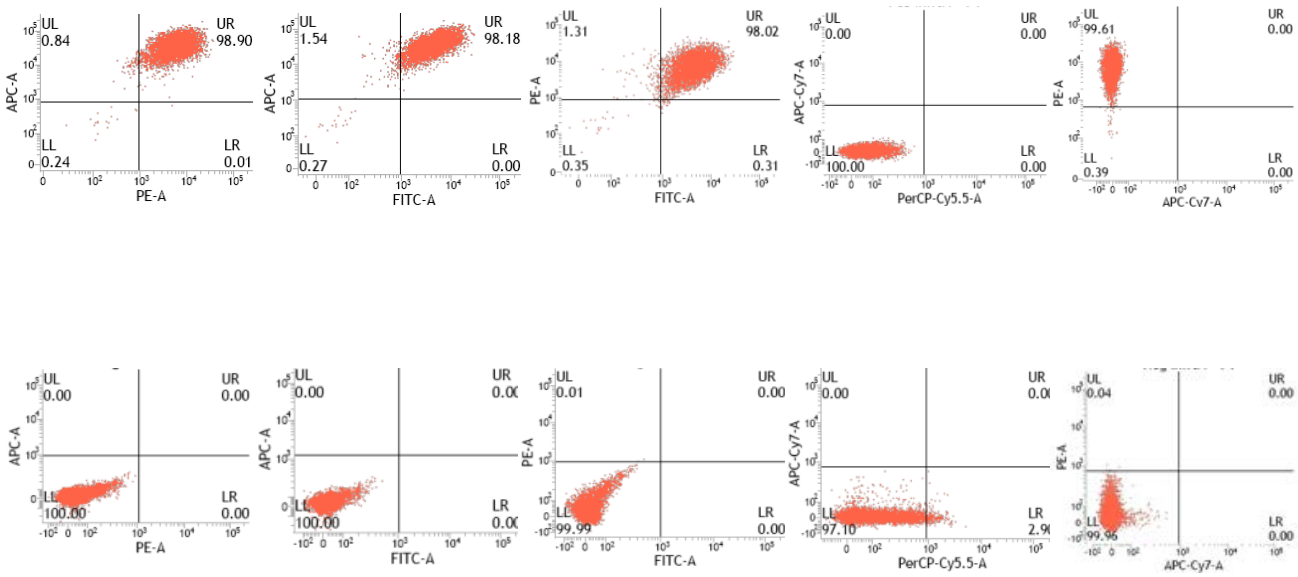

Figure 1: Flow cytometry of IMSCs(case No.4); First row shown positive markers(CD90-FITC, CD105-PE and CD73-APC) and second row shown negative markers(CD34-APC, CD45-PE, HLADR-APC).

Colony forming unit evaluation

After ASCs were cultured in polypropylene 6-well plates for 10 days then CFU counting had done (Figure 2). We found IMSCs had less of CFU's number (3.13±1.71 and 3.99±1.52) and size (9.91±4.72 and 3.99±1.52) than other group but non-statistical significantly different (P-value=0.428 and 0.263, respectively).

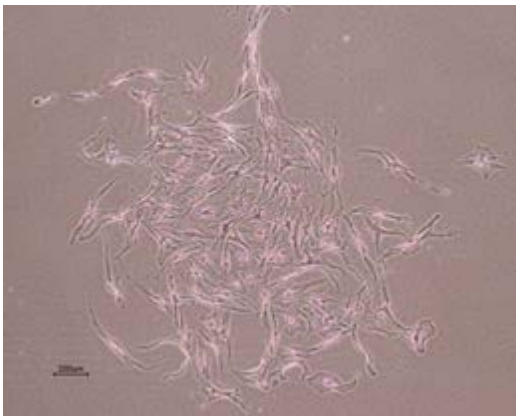

Figure 2: CFU of IMSCs(Case No.4) under light microscope(magnifier4x)

Safety assessment

All MSCs culture samples were not found bacterial or pathogen contamination from aerobe/anaerobe culture, PCR for mycobacterium, mycoplasma detection (official report by department of pathology, Ramathibodi hospital, 4 Dec 2014) and normal cell karyotypes (Figure 3).

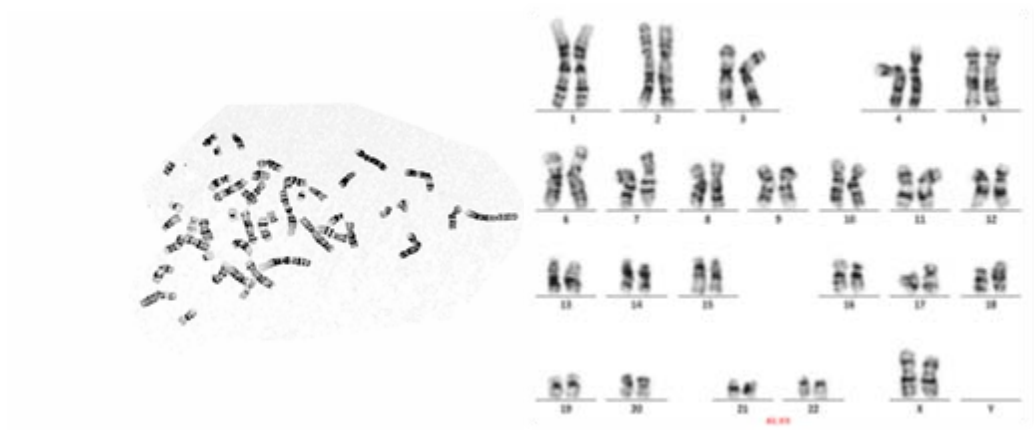

Figure 3: Normal karyotype of IMSCs (46, XX)

Table 2: Comparison of baseline characteristics between ASCs from infrapatellar fatpad and subcutaneous tissue

		Infrapatellar fatpad (N=5) n (%)	Subcutaneous (N=5) n (%)	P-Value
Gender				1.000†
Male		-	1(20.00)	
Female		5(100.00)	4(80.00)	
Age (yrs)*		65.80 ± 9.09	30.40 ± 13.16	0.001
BMI (kg/m^2)*		23.75 ± 3.23	23.52 ± 7.82	0.953
Weight of fat collection(gram)*		12.12 ± 2.57	49.75 ± 20.57	0.014
Number of ASCs isolation(P 0) ($x10^6$ cells/ml) *		3.98 ± 3.77	3.79 ± 1.75	0.923
Number of ASCs(P 0) per weight ($x10^4$cells/ml/gram) *		33.78 ± 31.07	9.28 ± 7.23	0.076‡
Incubation time to P 2 (days)*		18.80 ± 5.22	23.00 ± 7.52	0.341‡
Number of ASCs at P 2 ($x10^6$cells/ml)*		2.31 ± 1.24	2.43 ± 1.12	0.877
ASCs Markers				
Positive markers	CD 73(%)*	99.69 ± 0.26	99.60 ± 0.26	0.591
	CD 90(%)*	91.43 ± 10.79	93.85 ± 6.71	0.917‡
	CD 105(%)*	90.63 ± 9.49	87.85 ± 19.79	0.917‡
Negative markers	CD 34(%)*	1.24 ± 1.54	1.46 ± 2.22	0.917‡
	CD 45(%)*	0.17 ± 0.08	0.16 ± 0.12	0.882
	HLA-DR(%)*	0.55 ± 0.69	1.08 ± 2.01	0.834‡
Colony forming units (/100 cells)*		3.13 ± 1.71	3.99 ± 1.52	0.428
Size of CFU (mm^2)*		9.91 ± 4.72	12.99 ± 3.26	0.263

* Mean ± SD., † Fisher's exact test, ‡ Mann-Whitney U test

ASCs differentiation and histology

Pre-ASCs differentiation morphology detected under light microscope that flat polygonal cells were seen both groups. Post-ASCs differentiation in each cell lines, chondrogenic-/ adipogenic- and osteogenic induced, were staining by specific staining solution and shown positive staining both groups (Figure 4-6).

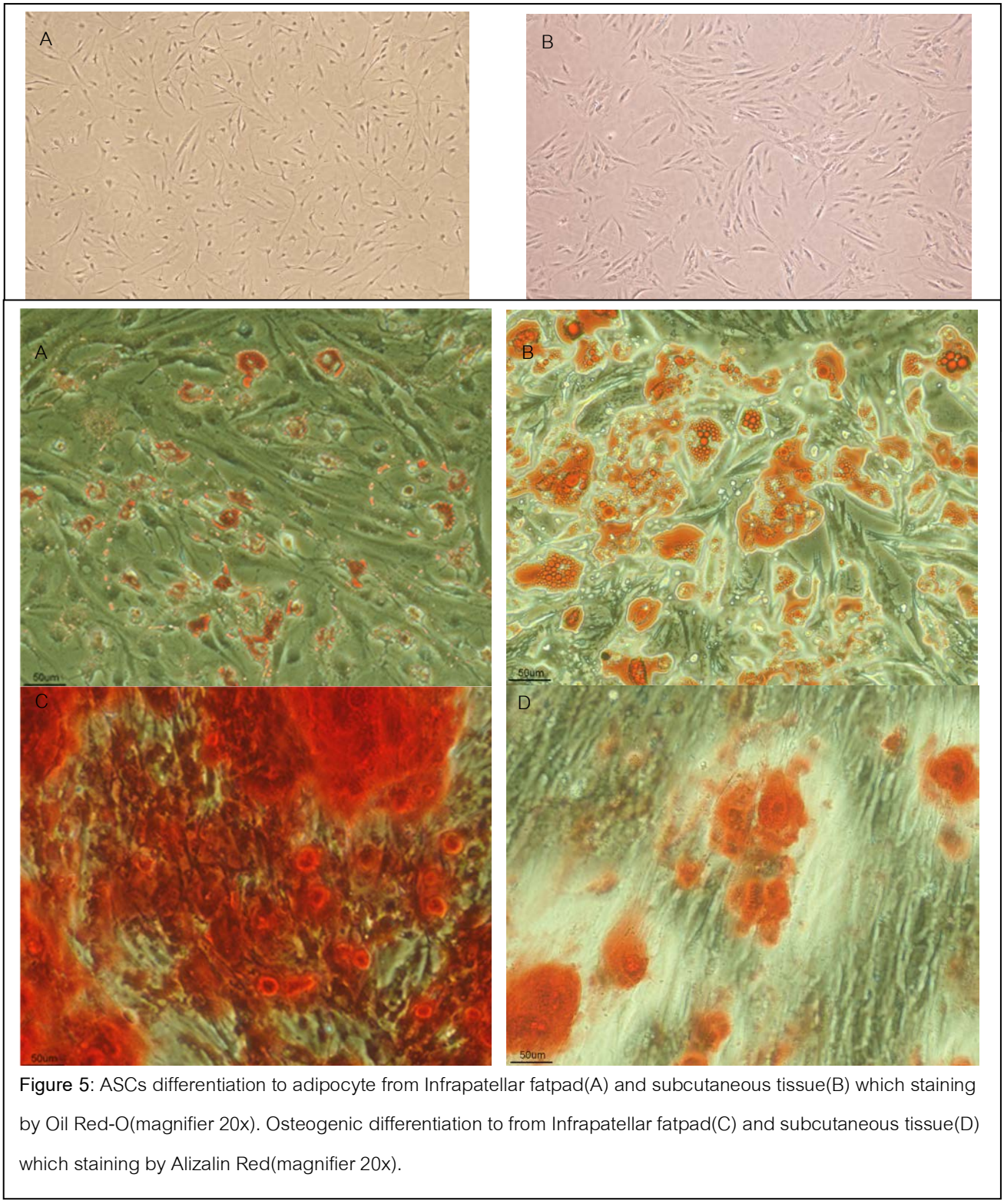

Figure 5: ASCs differentiation to adipocyte from Infrapatellar fatpad(A) and subcutaneous tissue(B) which staining by Oil Red-O(magnifier 20x). Osteogenic differentiation to from Infrapatellar fatpad(C) and subcutaneous tissue(D) which staining by Alizalin Red(magnifier 20x).

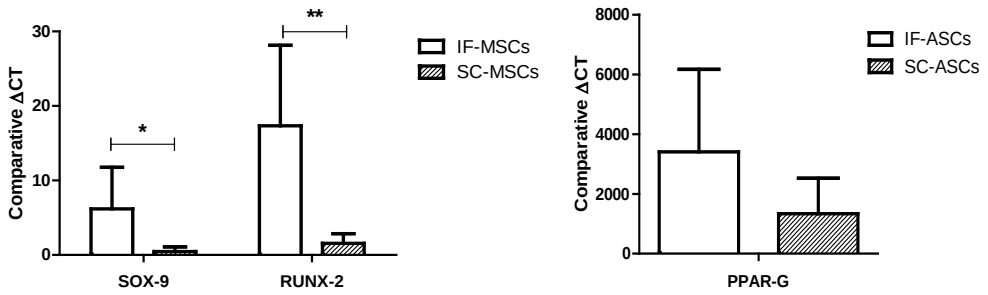

Figure 4(Left): Comparison of SOX-9 and RUNX-2 expression in IF-MSCs and SC-MSCs.

(Right): Comparison of PPAR-γ expression in IF-MSCs and SC-MSCs.

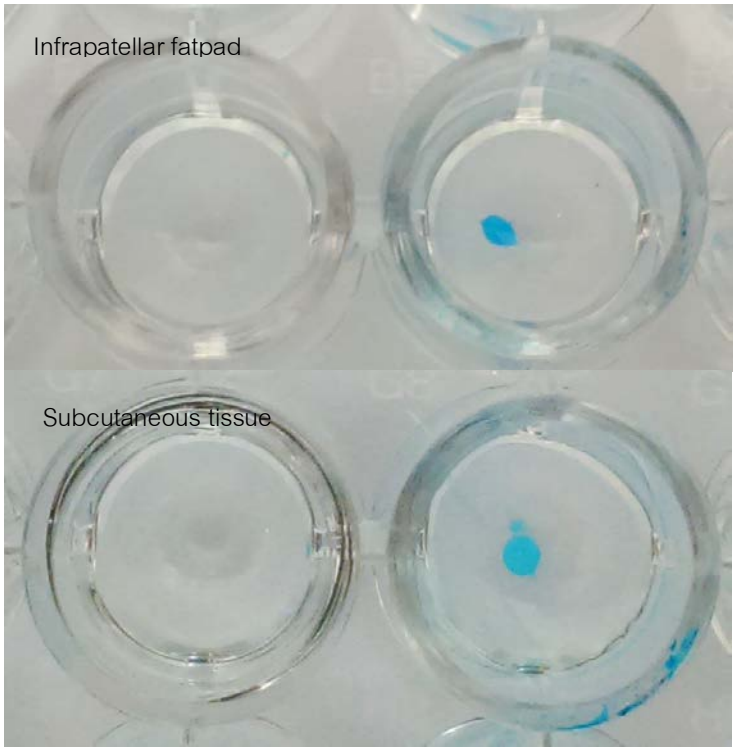

Figure 6: ASCs differentiation to chondrocyte from Infrapatellar fatpad and subcutaneous tissue which staining by Alcian Blue. Both groups shown blue staining the spheroid of chondrocyte.

(2) Gene express of growth and differentiation factor 5 in synovial tissue (objective 3)

Demographic data

There were 30 OA knee patients who underwent Total knee arthroplasty procedure included in this study. The severity of radiographic appearance was classified according to the KL score into KL3 (n=15) and KL4 (n=15). Baseline characteristics of the patients between the KL3 and KL4 groups including sex, age, onset of the disease, BMI, history of labor work, excessive kneeling activity, smoking and WOMAC score showed no statistical difference (Table 3).

Level of Gene expression in the different severity of OA knee

The level of GDF-5 gene expression using real time PCR between the radiographic severity groups showed a statistically significant difference in gene expression with median expression folds of 1.81 (0-9.46) and 3.5 (1.45-13.62) for the KL3 and KL4 group respectively (p-value = 0.0327) (Table 4).

Radiographic severity and Degree of synovititis

Selected synovial tissue of 10 samples from knee OA patients (n=5 for KL3 and n=5 for KL4) were determined their general histomorphlogy and graded for their degree of synovitis. The synovial tissue samples both the KL3 and the KL4 groups showed low-grade synovitis in hematoxylin and eosin stain (Table 5) with 2 or 3 layers of the synovial lining cells and slight increase in cellularity (Figure 6 Lt) and some infiltration of the inflammatory cells (Figure 6 Rt). There was no statistical difference in the synovitis score between both groups.

Table 3. Baseline characteristics between KL groups

Patient characteristics	KL grading scale		P-value
	KL3 (n = 15)	KL4 (n = 15)	
Sex			
Male No.(%)	3 (0.2)	1 (0.07)	0.6
Female No.(%)	12 (0.8)	14 (0.93)	
Age			
Mean (SD**)	68.73 (10.03)	64.53 (7.53)	0.21
range	53 - 83	50 - 77	
Onset of disease			
Mean (SD)	62.07 (10.5)	55.87 (7.54)	0.07
range	46 - 81	45 - 67	
BMI			
Mean (SD)	27.8 (6.38)	29.7 (5.58)	0.39
range	21.2 - 41	19.6 - 39.2	
History of labor work			
Yes (%)	2 (0.13)	1 (0.07)	1.0
No (%)	13 (0.87)	14 (0.93)	
Excessive kneeling activity			
Yes (%)	0 (0)	1 (0.07)	1.0
No (%)	15 (100)	14 (0.93)	
Smoking			
Yes (%)	1 (0.07)	2 (0.13)	1.0
No (%)	14 (0.93)	13 (0.87)	
WOMAC score			
Mean (SD)	119.6 (43.29)	126.4 (42.47)	0.67
range	55 - 184	46 - 189	

Table 4. GDF5 expression between KL groups

GDF5 expression (folds)	KL grading scale		P-value
	KL3 (n = 15)	KL4 (n = 15)	
Median (MAD) range	1.81 (0.92) 0 - 9.46	3.5 (1.59) 1.45 - 13.62	0.0327

Table 5. Synovitis grading between KL groups

Synovitis grading	KL grading scale	
	KL3 (n = 5)	KL4 (n = 5)
No synovitis (%) Low-grade synovitis (%) High-grade synovitis (%)	- 5 -	1 4 -

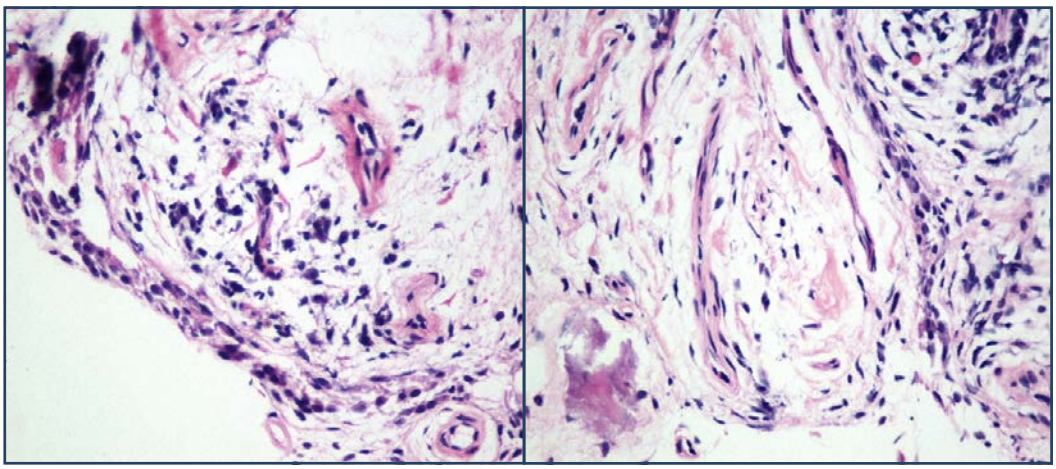

Figure 6. The synovial lining cells that form 2-3 layers with cellularity slightly increased (Lt) and few inflammatory cells infiltration (Rt)

(3) Evaluation differentiation TGF-b signal pathway of ASCs from subcutaneous and infrapatellar knee during chondrogenic differentiation (objective 3)

Members of the transforming growth factor beta (TGFβ) superfamily of secreted factors play essential roles and contribute to the development of cartilage formation and maintenance. The expression of genes related to TGF-Beta Pathway was determined using TGFß / BMP Signaling Pathway Plus RT2 Profiler PCR Array. The findings showed an up-regulation of genes related to

TGFb BMP Signaling Pathway including Pathway Activity Signature Genes, TGF beta superfamily Ligands, TGF beta Superfamily receptors, Transcription Factors and Regulators and SMAD Target genes in the IF-MSCs. **Table 6** shown the fold change of targeted genes in IF-MSCs compare to SC-MSCs.

Table 6 the TGF-b signal pathway related genes from IF-MSCs compared to SC-MSCs

Pathway Activity Signature Gene		
Gene	**Fold change**	**Sig.**
PMEPA1	3	P<0.001
THBS1	2.53	P<0.01
KLHL24	2.72	P<0.001
STK38L	14.27	P<0.001
SERPINE1	2.42	P < 0.05
FAS	2.35	P < 0.05
TGF beta superfamily Ligans		
Gene	**Fold change**	**Sig.**
BMP3	8.79	P<0.001
GDF5	2.94	P<0.001
TGFB3	2.74	P<0.001
BMP6	4.72	P<0.001
TGF beta Superfamily receptors		
Gene	**Fold change**	**Sig.**
ACVRL1	5.57	P<0.001
ACVR2A	9.19	P<0.001
Transcription Factors and Regulators		
Gene	**Fold change**	**Sig.**
MYC	4.95	P<0.001
PDGFB	6	P<0.001
SMAD Target genes		
Gene	**Fold change**	**Sig.**
IFRD1	2.52	P<0.01
ID1	3.21	P<0.001
COL1A1	5.06	P<0.001
BMPER	5.02	P<0.001

(4) Determine the animal models (Establish an appropriated model) (objective 4)

Time course for development of OA-related pain

At one-week post-surgery, a maximal level of change in the %HLWD was clearly observed in each experimental group except for the naïve group, in which a significant reduction in the mean %HLWD was observed in both surgically-induced OA groups compared to sham group (Fig.7). In addition, no significant difference in the mean %HLWD was noted at this period between these two models. Interestingly, the mean %HLWD in the rat osteochondral injury group was returned to the pre-operative status within 3-weeks post-surgery. However, this was not observed in the ACLT group, in which the mean %HLWD was partially reversed and remained significantly lower than those sham and osteochondral injury groups throughout the study period.

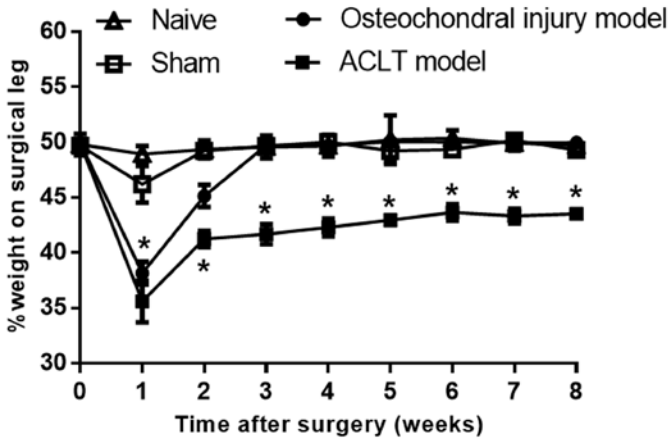

Figure 7. Percentage of weight on a surgical leg

Histopathological evaluation in the articular cartilage

Histopathological changes were assessed from H&E stained sections obtained from the rat femoral condyle. These changes were determined in parallel with the time course for development of pain behaviour. No changes were observed in the quality of cartilage for both naïve and sham groups at 12 weeks post-surgery, in which the surface of the articular cartilage is smooth with normal distribution of cartilaginous cells and intact osteochondral junction (Fig. 8a & 8b). For the ACLT group, histopathological changes in the articular cartilage surfaces were observed such as surface discontinuous with cloning of chondrocytes in transitional zone (Fig.8c), vertical fissure caused by erosion extended to transitional zone (Fig.8d), and extensive erosion, loss of matrix and hypocellularity chondrocytes (Fig.8e) at 4, 8 and 12 weeks post-surgery, respectively. Interestingly, it

was observed that the histopathological changes in the articular cartilage surfaces observed in the osteochondral injury model was different from the ACLT model. These changes include surface irregularity and disorientation chondrocytes (Fig.8f), erosion of superficial layer with hypocellularity chondrocytes (Fig.8g) and reparative tissue with fibrocartilage formation (Fig.8h) at 4, 8 and 12 weeks post-surgery, respectively.

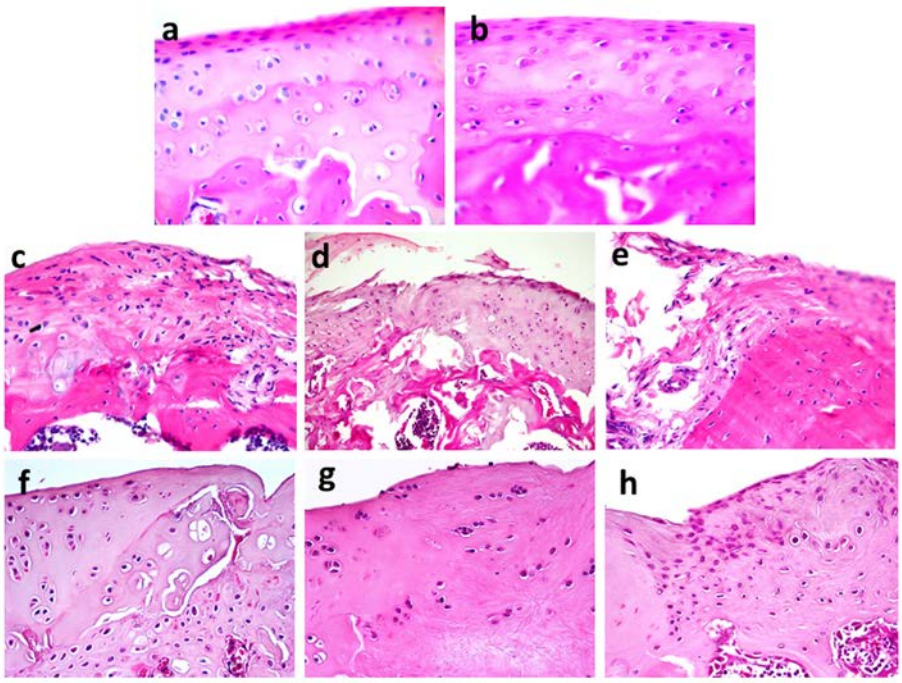

Figure8. H&E histological sections of rat femoral condyle 100x. Sections were score with OARSI scale. (a) Good quality cartilage of Naïve 15 weeks. The surface is smooth without irregularity and intact osteochondral junction. (b) Sham 15 weeks. Also show smooth surface with normal distribution of cartilaginous cells. (c) Surface discontinuous with cloning of chondrocytes in transitional zone of ACL model 4 weeks (d) Erosion causes vertical fissure extended to transitional zone of ACL model 8 weeks. (e) Extensive erosion, loss of matrix and hypocellularity chondrocytes of ACL model 12 week. (f) Surface irregularity and disorientation chondrocytes of Osterochondral defect 4weeks. (g) Erosion of superficial layer with hypocellularity chondrocytes of Osteochondral defect 8 weeks. (h) Reparative tissue with fibrocartilage formation of Osteochondral defect 12 weeks.

These changes were further evaluated by using the OASRI histopathology score. The mean (±SEM) OASRI scores for the ACLT group, observed at 4, 8 and 12 weeks post-surgery were 7.2 ± 0.7 (n=5), 10.5 ± 1.0 (n=6) and 15.2 ± 0.6 (n=6), respectively (Fig. 9a). A significant difference ($p<0.05$) in the OASRI score was also observed at 12 weeks compared with those observed at 4 and 8 weeks post-surgery. In contrast to ACLT group, no significant difference in the mean (±SEM) OASRI scores was observed among all study period groups post-surgery obtained from the osteochondral defect group, suggesting that osteochondral defect did not contribute to the progression of OA in this model. In addition, the results from histology grading also revealed that the defect areas obtained from the ACLT animals were in between stage 3 (25-50% involvement) and stage 4 (>50%

involvement), while the defect areas observed in the osteochondral injury animals were only in between 10-25% (stage 2 and 3).

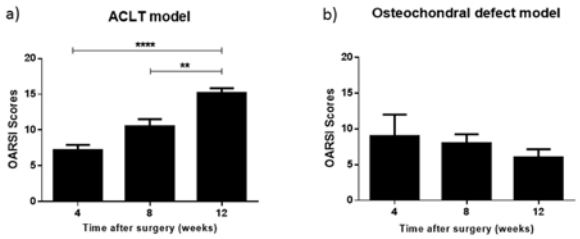

Figure 9. OARSI scores obtained from the ACLT model group and osteochondral defect model group at different study time points, including at 4, 8 and 12 weeks post-surgery. Values were expressed as mean ± SEM, ** $p < 0.01$ and **** $p < 0.0001$.

Moreover, the severity of OA progression in both models was also evaluated, in which the OASRI scores of both models were compared at the end of the follow up period (12 weeks post-surgery). There was a significance difference ($p < 0.05$) in the mean (±SEM) OASRI scores between both models and the sham and naïve groups. In addition, the mean (± SEM) OASRI of ACLT model was significant higher than those of osteochodral injury model (15.2 ± 0.6 and 6.0 ± 1.2) (Fig. 10).

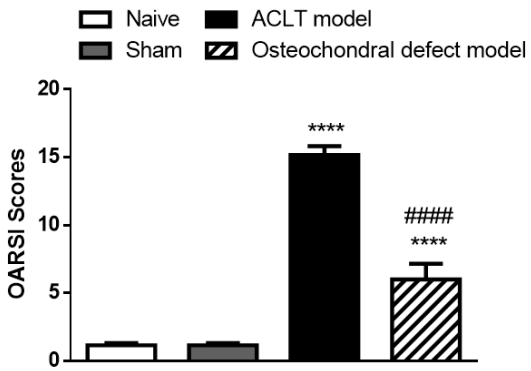

Figure 10 OARSI scores obtained from the ACLT model group and osteochondral defect model group at the end of the follow up period. Values were expressed as mean ± SEM, **** $p < 0.0001$.

(5) Comparative analysis of the alternative source of ASCs in a rat model of osteochondral defect: IF-ASCs VS. SC-ASCs (objective 4)

After 21 days of culture in chondrogenic media, both IF-ASCs and SC-ASCs cartilage constructs displayed round with white opaque color in which more solid texture was noted for IF-ACSs (Fig. 11). Histologically, staining of these cartilage constructs with H&E revealed cells with fibroblast-like structure, in which they were surrounded by an abundant extracellular matrix. In addition, the results also revealed that both cartilage constructs stained strongly for type II collagen and slightly for aggrecan when compared with IgG isotype controls (Fig. 12). Both cartilage construct was implanted into an osteochondral model. The model was selected from the previous experiment.

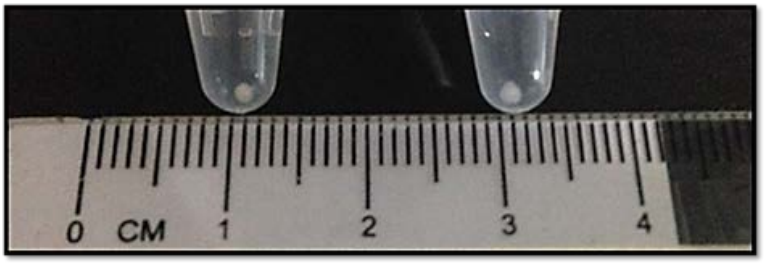

Figure 11 3D cartilage constructs of adipose-derived mesenchymal stem cells from subcutaneous adipose tissue (SC-ASCs) (Left) and infrapatellar fat pad (IF-ASCs) (Right).

.

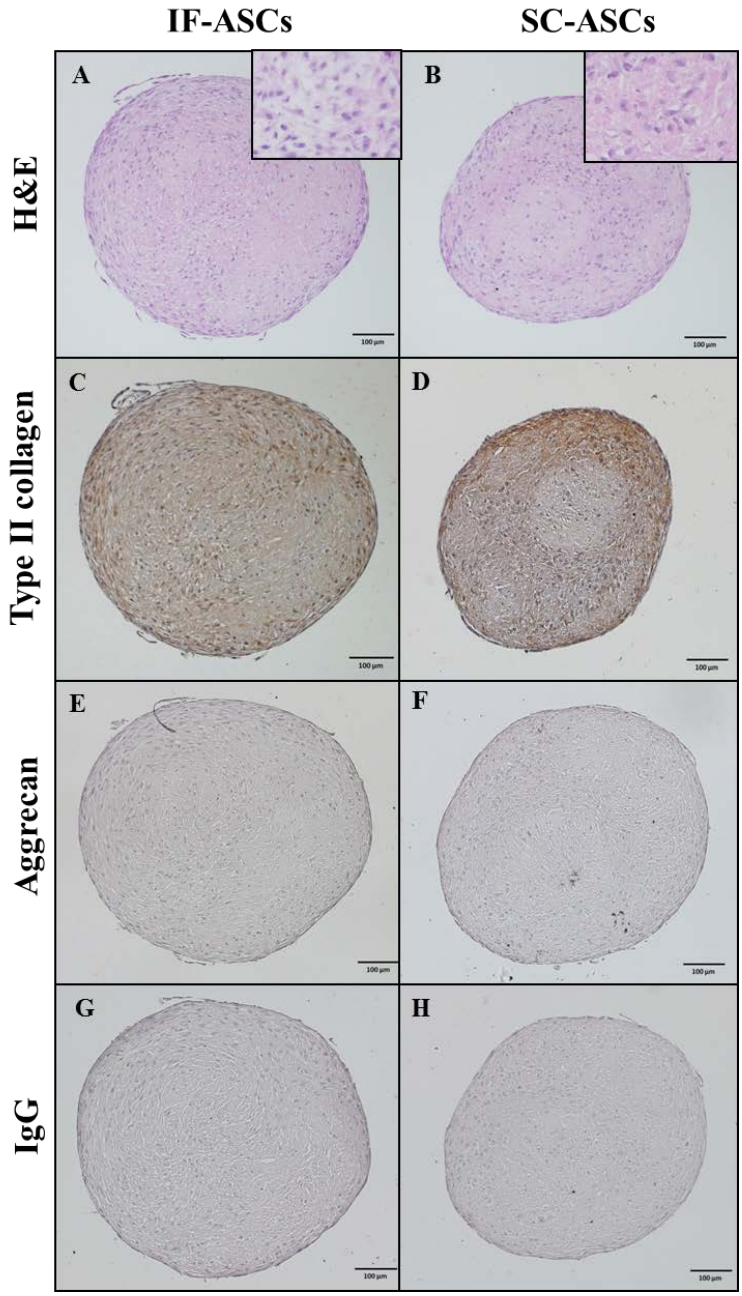

Figure 12 Immunohistochemistry staining of 3D cartilage constructs of IF-ASCs, SC-ASCs and IgG staining as controls. H&E staining: representative images of cells with round morphology (A, B). Immunohistochemical analyses of cartilage constructs of IF-ASCs and SC-ASCs: representative IHC images showed strongly stained for type II collagen (C, D) and slightly stained for aggrecan (E, F). Negative control of IHC: IgG isotype (G, H). Magnification 10✕. Scale bars at 100 μm as indicated.

After 4 weeks of implantation, there was no marked difference at the surface appearance of defects implanted with either IF-ASCs or SC-ASCs. In addition, gross observations revealed that both implanted defects were almost completely filled with cartilaginous white tissue. However, they could still be clearly distinguished from surrounding areas, suggesting an improvement of the repaired defect regardless of their source of origin (Fig. 13 A). For histological examinations, it was found that the portion of both IF-ASCs and SC-ASCs cartilage constructs can

clearly be seen and remained in the defect region after 4 weeks of implantation. The viability of cells in the constructs can also be observed as evidenced by the presence of nuclear material (Fig. 13 B, C). Moreover, immunohistochemical staining for type II collagen revealed that most of these cells are mature chondrocytes which exhibited a chondrocytic phenotype, including large round cells encapsulated in lacunae. The reparative tissues showed a combination of flattened fibrous tissue and mature chondrocytes. The existence of differentiated chondrocytes surrounded by type II collagen matrix was well-defined in IF-ASCs and SC-ASCs groups. Interestingly, chondrocytes were markedly seen to be in columns-oriented distribution in IF-ASCs (Fig. 13 D, E) compared to those in SC-ASCs. Consistent with type II collagen, there **was also** a **more intense of immunostained for** aggrecan in IF-ASCs constructs than those in SC-ASCs (Fig. 13 F, G). Despite of this, no significant difference in the histological scoring between two sources of constructs were observed (Fig. 14). Similarly, the quantitative measurement of immunostaining for type II collagen and aggrecan also revealed that no significant differences were also observed between these constructs (Fig. 15).

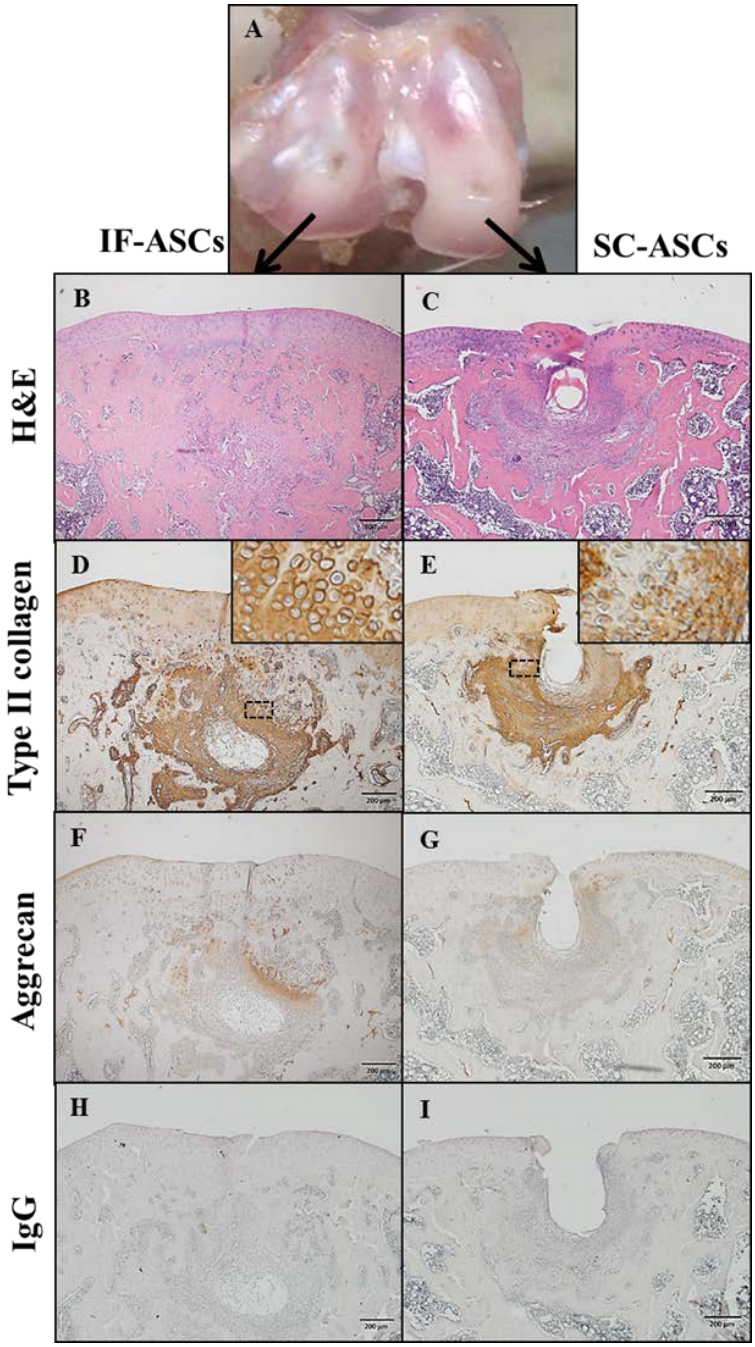

Figure 13 Macroscopic observations and histological examination of IF-ASCs and SC-ASCs at 4 weeks post-implantation. Gross appearance showed a slightly rough surface of the femoral condyle regardless of the source of ASCs (A). H&E (B, C), type II collagen (D, E) and aggrecan (F, G) staining of tissues IgG isotype (H, I). Magnification 4✕. Scale bars at 200 μm as indicated.

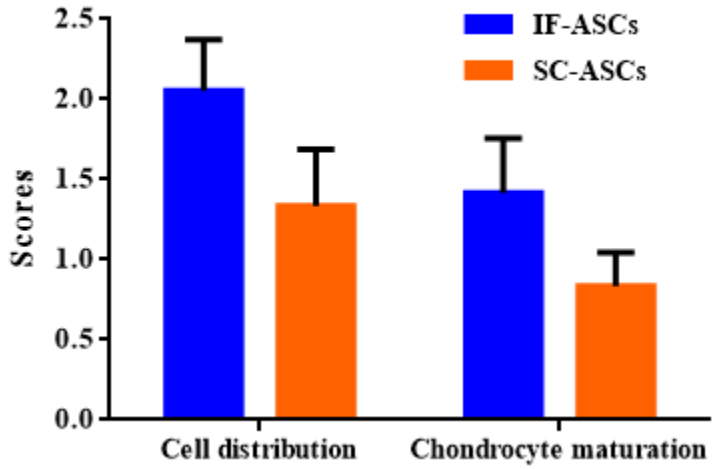

Figure 14 Histological grading scores of the regenerated tissue in the repaired osteochondral defect. Results from IF-ASCs (n = 6) and SC-ASCs (n = 6) groups are shown. All data were expressed as the mean and SEM.

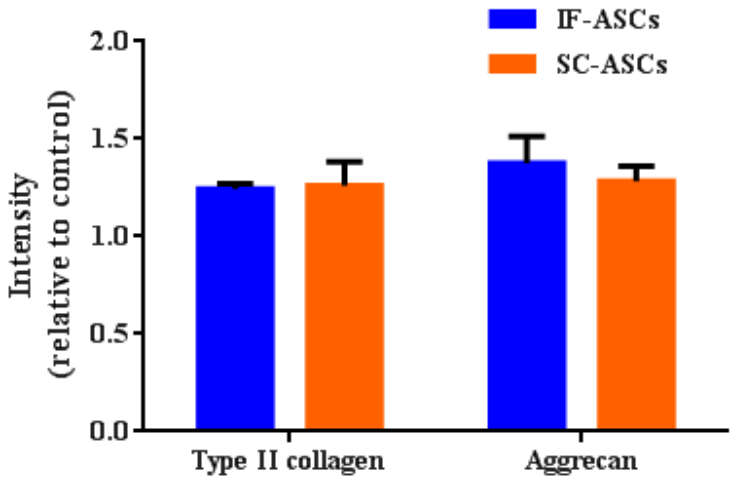

Figure 15 The quantitative measurement of immunohistochemistry staining for type II collagen and aggrecan. Results from IF-ASCs (n = 6) and SC-ASCs (n = 6) groups are shown. All data were expressed as the mean and SEM.

Discussion and Further research:

Many in vitro studies have recently been reported the application of ASCs for hyaline cartilage regeneration. However, to our knowledge, only limited in vivo study is available that compared the chondrogenic differentiation characteristics as well as the ability to regenerate damaged hyaline cartilage between ASCs that harvested from IF and SC. Therefore, the major aim of the present study was to investigate whether scaffold free cartilage construct of IF-ASCs and SC-ASCs can enhance the regeneration of hyaline cartilage.

This study was focused on ASCs preparation from 2 different sources, namely subcutaneous tissue (SC) and infrapatellar fatpad (IPFP). Their sterility and karyotype were evaluated in this study to ensure for safety concerns. There was no contamination during the process of cell isolation and culture expansion. For their general morphology, they were exhibited fibroblast liked appearance and plasticity in both groups with no significant difference. Their cell surface profiles demonstrated by flow cytometry assessment CD 73, 90, 105 for positive markers and CD 34, 45, HLA-DR for negative markers, those were similar in both groups. Their proliferation potentials were evaluated using cologenicity and chronogenicity by number and size of CFUs. The results were shown no difference between both groups. For evaluation of their differentiation abilities, ASCs from IPFP source showed superiority in the osteogenic and chondrogenic differentiation than SC source demonstrating by SOX-9 and RUNX-2 expression which in represents for chondogenic-differentiation pathway, andosteogenic-differentiation pathway, respectively. Thus, it is assumed from in vitro study that infrapatellar may be a good candidate source for cartilage regeneration.

Moreover, it was demonstrated that hyaline cartilage could be successfully regenerated in a rat model of osteochondral defect by implantation with scaffold free cartilage constructs of either IF-ASCs or SC-ASCs. The chondrogenic differentiation characteristics of these constructs were first confirmed prior to implantation by determining the expression of SOX-9 and COL2A1 genes. In the present study, it was revealed that scaffold free cartilage constructs of IF-ASCs exhibited superior SOX-9 expression compared to those of SC-ASCs. However, the current finding did not see any significant difference in the COL2A1 expression between IF-ASCs and SC-ASCs. One possible explanation for this inconsistent finding might be due to the difference in the expression level of COL2A1 which was obtained from different sources. The present study, SC was harvested by liposuction from patients who received cosmetic surgery whereas in the previous study obtained SC from knee. Another possibility could be due to a limited number of donors in the present study. Histologically, staining of both IF-ASCs and SC-ASCs constructs with H&E revealed cells with fibroblast-like appearance, which they were surrounded by an abundant extracellular matrix as indicated by immunostaining with collagen type II and aggrecan. This result suggested that the cartilage constructs obtained from both sources can produce type II collagen and proteoglycans matrix, which are the main components in the articular cartilage, confirming their chondrogenic differentiation ability. Based on these results together with the concomitant increase in the expression of SOX-9 and type II collagen protein in both constructs, these data confirmed the chondrogenic differentiation potential of both constructs.

After the chondrogenic differentiation potential of both IF-ASCs and SC-ASCs constructs was confirmed and compared in an in vitro study, further investigation in an in vivo was performed to investigate whether their differentiation potentials can be retained after implantation into an osteochondral defect of the rat knee for 4 weeks. One important question might be raised concerning the viability of the cells in cartilage constructs that were implanted into defect site of the animal, particularly in the middle part of the constructs. The H&E staining results revealed that most cells in the constructs were viable as indicated by the presence of a nucleus and absence of apoptotic cells.

The present results also observed cartilage lacunae, which are the indicative of mature chondrocytes, in the implanted of both constructs as well as the surrounding repaired area after 4 weeks of implantation. These data suggested that the immature chondrocytes with fibroblast-like structure that were observed in the constructs can differentiate into mature chondrocytes via chondrogenesis process after implantation. This chondrogenic differentiation ability of the constructs after implantation was also confirmed by a positive immunostaining for type II collagen and aggrecan. Moreover, the present finding also found that the mature chondrocytes in the IF-ASCs constructs were markedly arranged in column-oriented compared to SC-ASCs constructs. This may be explained by the fact that IF-ASCs construct has a higher expression level of SOX-9 protein than that of SC-ASCs construct. Despite of this, no significant difference in the histological scoring and intensity level of immunohistochemistry staining was observed, suggesting that the regeneration of hyaline cartilage can be enhanced by implantation with the scaffold free cartilage constructs of ASCs derived from either IF or SC-ASCs. Based on the above finding, this study demonstrated that both IF-ASCs and SC-ASCs constructs can retain their chondrogenic differentiation potential as well as enhancing the hyaline cartilage regeneration after implantation for 4 weeks.

Further study, IF-ASCs constructs were used for implantation to further investigate their regenerative potential in large animal such as rabbit. More explanation in the mechanisms for IF-ASCs construct based on its ease of harvest and a higher chondrogenic potential than those of SC-ASCs construct should be further investigated.

Conclusion:

In summary, this study demonstrated that scaffold free cartilage constructs of either IF-ASCs or SC-ASCs can be successfully implanted into the osteochondral defect of rat model and retained for up to 6 weeks post-implantation. This provided novel and interesting insights into their differentiation ability to support the current hypothesis that human 3D cartilage construct obtained from adipose tissues may be used as an alternative source to repair the cartilage defect and IF-ACSs should be considered as the potential source and could be used for cellular based therapy for cartilage injury.

เอกสารแนบหมายเลข 3

Output จากโครงการวิจัยที่ได้รับทุนจาก สกว.

1. ผลงานตีพิมพ์ในวารสารวิชาการนานาชาติ

ได้รับการตีพิมพ์ผลงานในวารสารระดับนานาชาติ 1 เรื่อง
T. Tawonsawatruk, O. Sriwatananukulkit, W. Himakhun, W. Hemstapat. Comparison of pain behaviour and osteoarthritis progression between anterior cruciate ligament transection and osteochondral injury in rat models. Bone Joint Res 2018; 7:244–251.

2. การนำผลงานวิจัยไปใช้ประโยชน์

ในเชิงวิชาการสามารถใช้เป็นแหล่งอ้างอิงในการวิจัยเกี่ยวงานวิจัยด้านออร์โธปิดิกส์ อีกทั้งทางศูนย์วิจัยคณะแพทย์ศาสตร์รามาธิบดี ยังได้ใช้ผลงานวิจัยดังกล่าวในการพัฒนารูปแบบการจัดเก็บเซลล์ต้นกำเนิดที่สกัดจากสกัดได้จากเนื้อเยื่อไขมันใต้เข่า เพื่อเป็นแหล่งข้อมูลในการต่อยอดการวิจัยที่เกี่ยวข้องในอนาคต และผลการวิจัยส่วนหนึ่งใช้ใน การประสานความร่วมมือทางวิชาการและการวิจัย ระหว่าง คณะแพทยศาสตร์โรงพยาบาลรามาธิบดี กับ Osaka University, Japan

Follow us @BoneJointRes

Freely available online OPEN ACCESS

BJR

OSTEOARTHRITIS

Comparison of pain behaviour and osteoarthritis progression between anterior cruciate ligament transection and osteochondral injury in rat models

T. Tawonsawatruk, O. Sriwatananukulkit, W. Himakhun, W. Hemstapat

Department of Pharmacology, Faculty of Science, Mahidol University, Bangkok, Thailand

Objectives

In this study, we compared the pain behaviour and osteoarthritis (OA) progression between anterior cruciate ligament transection (ACLT) and osteochondral injury in surgically-induced OA rat models.

Methods

OA was induced in the knee joints of male Wistar rats using transection of the ACL or induction of osteochondral injury. Changes in the percentage of high limb weight distribution (%HLWD) on the operated hind limb were used to determine the pain behaviour in these models. The development of OA was assessed and compared using a histological evaluation based on the Osteoarthritis Research Society International (OARSI) cartilage OA histopathology score.

Results

Both models showed an increase in joint pain as indicated by a significant ($p < 0.05$) decrease in the values of %HLWD at one week post-surgery. In the osteochondral injury model, the %HLWD returned to normal within three weeks, while in the ACLT model, a significant decrease in the %HLWD was persistent over an eight-week period. In addition, OA progression was more advanced in the ACLT model than in the osteochondral injury model. Furthermore, the ACLT model exhibited a higher mean OA score than that of the osteochondral injury model at 12 weeks.

Conclusion

The development of pain patterns in the ACLT and osteochondral injury models is different in that the OA progression was significant in the ACLT model. Although both can be used as models for a post-traumatic injury of the knee, the selection of appropriate models for OA in preclinical studies should be specified and relevant to the clinical scenario.

Cite this article: *Bone Joint Res* 2018;7:244–251.

Keywords: Surgically induced osteoarthritis model, Anterior cruciate ligament transection, Osteochondral injury, Pain, Osteoarthritis progression

Article Focus

- The comparison of pain behaviour and osteoarthritis progression between anterior cruciate ligament transection (ACLT) and osteochondral injury in a rat model.

Key Messages

- The pain behaviour patterns developed differently in the ACLT and osteochondral injury models.
- Certain types of knee injury can affect the progression of osteoarthritis (OA), in which more severe OA tended to develop in the ACLT model than in the osteochondral injury model.

Strengths and limitations

- The different types of knee injury models in rats, including ACLT and osteochondral injury models, were directly compared in terms of the pain behaviour and OA progression.
- This study has demonstrated only the pain pattern and the OA progression, however, the underlying mechanisms that caused these differences have not been determined to date.

T. Tawonsawatruk, MD, PhD, Assistant Professor, Department of Orthopedics, Ramathibodi Hospital, Mahidol University, Bangkok, Thailand.

O. Sriwatananukulkit, MSc, PhD student,

W. Hemstapat, PhD, Assistant Professor, Department of Pharmacology, Faculty of Science, Mahidol University, Bangkok 10400, Thailand.

W. Himakhun, MD, Assistant Professor, Department of Pathology and Forensic Medicine, Faculty of Medicine, Thammasat University, Pathumthani 12120, Thailand.

Correspondence should be sent to W. Hemstapat; email: warinkarn.hem@mahidol.ac.th

doi: 10.1302/2046-3758.73.BJR-2017-0121.R2

Bone Joint Res 2018;7:244–251.

Introduction

Osteoarthritis (OA) commonly affects the weight-bearing joints,[1] and is associated with articular cartilage degeneration and subchondral bone sclerosis at the joint margins.[2] The common clinical features of OA include joint pain, swelling, stiffness and crepitation, with loss of joint function that results in a reduced quality of life in patients.[3] In approximately 12% of patients, OA may be secondary to an underlying condition, including prior joint injury, abnormal mechanical loading (i.e. bowed legs), an inflammatory arthropathy such as gout, and metabolic conditions such as diabetes. In addition, OA may be secondary to trauma, and injury to the joint is either by direct cartilage injury, or disruption to the ligamentous stabilizers of the joint, and may be one of the aetiologies of post-traumatic secondary OA.[4,5]

Initially, OA changes in the joint may be asymptomatic, and it may take some years for either symptoms or physical signs to become evident. A variety of animal models have been developed to enable investigators to study the development of OA over a limited time scale.[6,7] Animals of various species have been investigated and the pathological features observed in human OA can be replicated in the animal model.[6-8] However, no single model is sufficient to reproduce all aspects of the pathology of human OA.[6] Animal OA models can be broadly classified into three groups, including naturally occurring (i.e. a spontaneous disease), chemically-induced, and surgically-induced joint instability models.[9,10]

As secondary OA is often post-traumatic, surgically-induced OA models, such as those of anterior cruciate ligament transection (ACLT), and osteochondral injury, were used in this study to mimic human joint trauma. The ACLT model is one of the most widely used, and may reproduce the post-traumatic OA changes, as reported in humans.[6,11] The anterior cruciate ligament (ACL) is one of the four primary stabilizers of the knee, and prevents anterior translation of the tibia.[12] In animals, OA can be surgically induced by transection of the ACL, which leads to symptomatic joint pain and structural joint changes. The ACLT model can be developed and reproduced in a variety of species, including rats, mice, guinea pigs, rabbits, cats, dogs, sheep and monkeys.[13] This model can demonstrate osteoarthritic features similar to those observed in human OA, including articular cartilage degradation, subchondral bone sclerosis and osteophyte formation.[14,15]

Cartilage or osteochondral injury is strongly associated with a higher incidence of OA.[16] Similar to an ACL injury, an osteochondral injury can be post-traumatic and may be the result of sports injuries or other accidents. There has been increased clinical interest in treating focal cartilage injuries to eliminate symptomatic joint pain and prevent the progression of OA.[17] Direct injury to the joint, including creation of a focal osteochondral defect, is a common method to induce cartilage loss, and can be used to investigate the treatment strategy for cartilage regeneration in preclinical studies.[18] However, there is little evidence of an osteochondral injury contributing to the progression of OA in an animal model, and so whether a localised cartilage injury can result in secondary OA changes, remains a controversial topic of debate.[19]

In recent years, various small animal models of OA have been established, and have been used in a number of studies to understand the pathophysiology of OA and to evaluate new treatment options for OA.[20,21] There is, however, a lack of information regarding the relationship between OA-related pain behaviour in surgically-induced OA models, and the progression of OA over time. While pain outcomes have not been described for osteochondral injury models, they have been reported for ACLT, including data on temporal patterns and its relationship to OA pathology. Thus, the objectives of this study were to compare the development of OA-related pain behaviour patterns and the histopathological progression of OA between these two animal models of OA. The findings of this study may help better to understand the clinical manifestation of articular pain and the natural history of different injury types regarding the progression of the secondary OA resulting from direct cartilage injury and ligament injury.

Materials and Methods

Experimental animals. The experimental protocols were approved by the Animal Ethics Committee at the Faculty of Science, Mahidol University of Thailand (Protocol No. 212 and MUSC58-009-324). The study was conducted on a total of 51 male Wistar rats at six weeks of age that weighed 140 g to 180 g at the time that the animals were received. The rats were obtained from the National Laboratory Animal Centre, Mahidol University, Thailand, and they were housed in pairs and allowed to acclimatize to the laboratory housing conditions for a week prior to starting the experimental procedures. The rats were kept in a temperature-controlled room (mean 20°C, SD 2°C) maintained at a mean humidity of 60% (SD 10%) with a 12-by-12-hour dark-light cycle. Standard laboratory rat food and water were supplied *ad libitum*.

Surgical procedure. Following anaesthesia using a mixture of xylazine (5 mg/kg, Thai Meiji Pharmaceutical Co. Ltd, Bangkok, Thailand) and Zoletil (40 mg/kg, Virbac Laboratories, Carros, France) administered by a single intraperitoneal injection, the surgical areas around the right knee joint were shaved and disinfected with povidone iodine. A longitudinal incision was made over the patella, and after blunt soft-tissue dissection, the medial side of the joint was opened with a scalpel and the patella was dislocated laterally to expose the femoral condyles. In the ACLT model, the ACL was transected (Fig. 1a) as previously described,[15,22,23] and the transection was

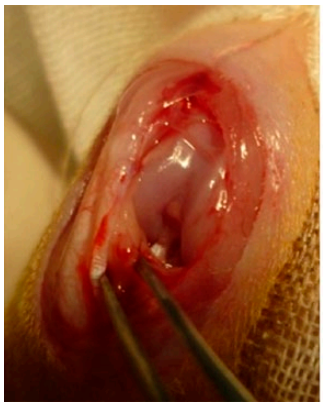

Fig. 1a

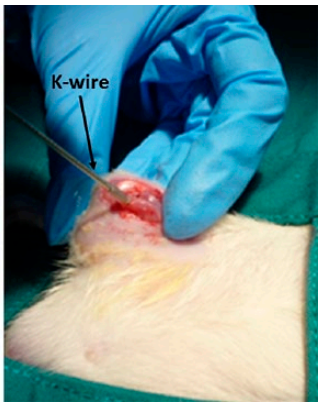

Fig. 1b

Images showing the induction of surgically induced osteoarthritis models: a) anterior cruciate ligament transection; b) osteochondral defect.

confirmed by an anterior drawer test.[23] For the osteochondral injury model, the injury was created using a 1.4mm diameter Kirschner (K-) wire to a depth of 3 mm in the medial femoral condyle, until it reached the bone marrow region (Fig. 1b).[24] Sham animals underwent the same operation as OA-induced animals, without transection of the ACL or an osteochondral injury. After the procedure, the wound was closed in layers with Vicryl 4-0 braided absorbable sutures and 4-0 silk sutures to the skin. (Ethicon, Livingston, United Kingdom). Cefazolin (Cefaben 20 mg/kg; L.B.S Laboratory Ltd, Part, Bangkok, Thailand) was administered via subcutaneous injection 30 minutes prior to surgery and every day after the procedure for four days to prevent postoperative infection.

Assessment of pain-related behaviour. A total of 31 male Wistar rats were randomly assigned into four groups: Group 1 - control naïve group (n = 6); Group 2- sham group (n = 7); Group 3- ACLT group (n = 10) and Group 4- osteochondral injury group (n = 8). The pain assessment was carried out weekly for up to eight weeks after operation using the hind limb weight-bearing test (Incapacitance meter; Columbus Instruments International, Columbus, Ohio). This technique measures the difference in weight bearing between the operated and non-operated contralateral limbs. Changes in the hind limb weight distribution (%HLWD) on the operated hind limb were used to determine the degree of knee joint pain. The %HLWD was determined as described previously.[22]

Tissue preparation and histopathological evaluation. In addition to the animals used in the pain-related behaviour study, an additional group of 20 male Wistar rats was obtained for histopathological study, and the animals were randomly assigned to four groups (n = 5/group) according to the animal model (ACLT or osteochondral defect groups) and experimental endpoints (4 or 12 weeks after surgery). Following the last pain assessment at week 8 for pain-related behaviour study, as well as at 4 and 12 weeks post-surgery for histopathological study, the animals were euthanized via intraperitoneal injection of thiopental (Nembutal, 100 mg/kg; Ceva Santé Animale, Libourne, France). The knee joints on the operated hind limb were collected for histopathological comparisons between the two surgically-induced models and control groups (naïve and sham) at each timepoint.

The knee joint on the operated hind limb was preserved in 10% neutral buffered formalin (NBF) for three days, and it was subsequently decalcified for three weeks in 10% ethylenediaminetetraacetic acid. The decalcified joints were then embedded in paraffin and cut into coronal sections of 4 µm to 5 µm through the medial tibial plateau surfaces. The tissue slides were stained with haematoxylin and eosin (H&E) to evaluate the general morphology of the joint cartilage. The histopathological progression of OA in all experimental groups was determined twice for each animal (one section per joint) by an experienced pathologist in a blinded manner, and the average of scores were used for analysis according to the Osteoarthritis Research Society International (OARSI) histopathology score.[25]

On each section, the following parameters were determined: matrix loss, cartilage degeneration, subchondral involvement and osteophytes. A multiplication of the assessment based on both the severity (grade) and extent (stage) of OA in the articular cartilage was calculated. The morphological features of articular surface were divided into seven grades, depending on the severity: Grade 0, normal and both matrix and cells are intact; Grade 1, superficial and intact with mild fibrillation; Grade 2, surface discontinuity; Grade 3, vertical fissures (clefts) involving the mid-zone; Grade 4, matrix loss/delamination of the superficial layer; Grade 5, denudation of the surface with subchondral bone involvement; and Grade 6, deformation of the joint. Grades 1 to 4 involve articular cartilage changes only, whereas grades 5 and 6 involve the subchondral bone.

The OA stages were defined according to the horizontal extent (width) of the involved cartilage surface irrespective of underlying OA grade. Based on the microscopic section, the representative involvement was as follows:

- Stage 1; < 10%
- Stage 2; 10% to 25%
- Stage 3; 25% to 50%
- Stage 4; > 50%.

In this study, the whole area of the tibial plateau was considered to be 100%. This score allowed standardization and comparison of results between two surgically induced OA models in the present study.

Statistical analysis. All data were expressed as the mean and standard error of the mean (SEM). Statistical significance was determined using one-way analysis of variance (ANOVA) followed by Tukey's *post hoc* test for

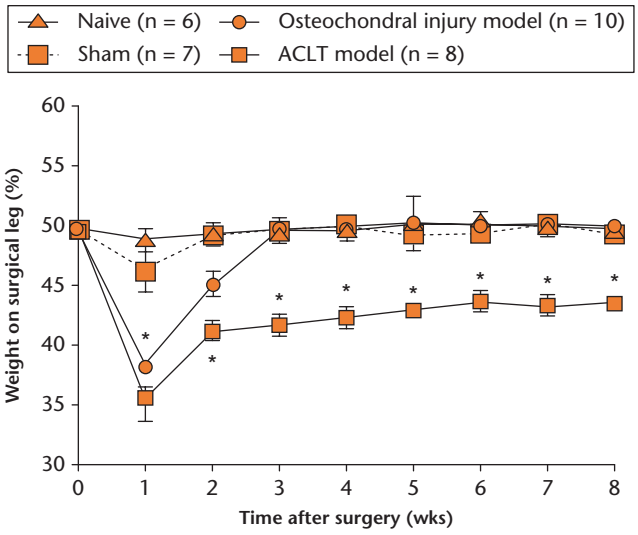

Fig. 2

Graph showing the course of time for the development of an osteoarthritis (OA)-related pain profile in surgically-induced OA models. The pain-related behavioural results were expressed as the mean percentage of weight-bearing distribution on the operated hind limb (*$p < 0.05$ *versus* sham and naïve groups). Each point represents the mean and standard error of the mean of each group. ACLT, anterior cruciate ligament transection.

multiple comparisons. Statistical analysis was performed with GraphPad Prism (La Jolla, California) (version 6.0). A p-value < 0.05 indicated a significant difference between groups.

Results

Time course for development of OA-related pain. One week after surgery, a maximal level of change in the %HLWD was clearly observed in each experimental group (except for the naïve group,) and a significant reduction in the mean %HLWD was observed in both surgically induced OA groups compared with the sham group (Fig. 2). This outcome was accompanied by a significant ($p < 0.05$) decline in the %HLWD of the ACLT group and osteochondral group, which decreased from 49.9% (SEM 0.2%) to 35.6% (SEM 1.9%) and from 50.0% (SEM 0.1%) to 38.2% (SEM 1.0%), respectively (Fig. 2).

There was no significant difference in the mean %HLWD at this one-week time period between the two models. After this, the mean %HLWD in the osteochondral injury group returned to its preoperative status within three weeks of surgery. In contast, this was not observed in the ACLT group (41.7%, SEM 0.9%), and the mean %HLWD remained significantly lower compared with the sham (49.6%, SEM 0.6%) and osteochondral injury (49.6%, SEM 0.5%) groups throughout the study period.

Histopathological evaluation in the articular cartilage. Histopathological changes were assessed from H&E-stained sections obtained from the femoral condyle. These changes were determined in parallel with the time course for the development of pain behaviour. No changes were observed in the quality of cartilage for either the naïve or sham groups at 12 weeks post-surgery, in which the surface of the articular cartilage is smooth with a normal distribution of cartilaginous cells and an intact osteochondral junction (Figs 3a and 3b). For the ACLT group, histopathological changes in the articular cartilage surfaces were observed, including delamination of the articular surface with cloning of chondrocytes in the transitional zone (Fig. 3c), a vertical fissure caused by erosion extending into the transitional zone (Fig. 3d), and extensive erosion, loss of matrix and hypocellularity chondrocytes (Fig. 3e) at four, eight and 12 weeks post-surgery, respectively. In the osteochondral injury group, different histopathological changes

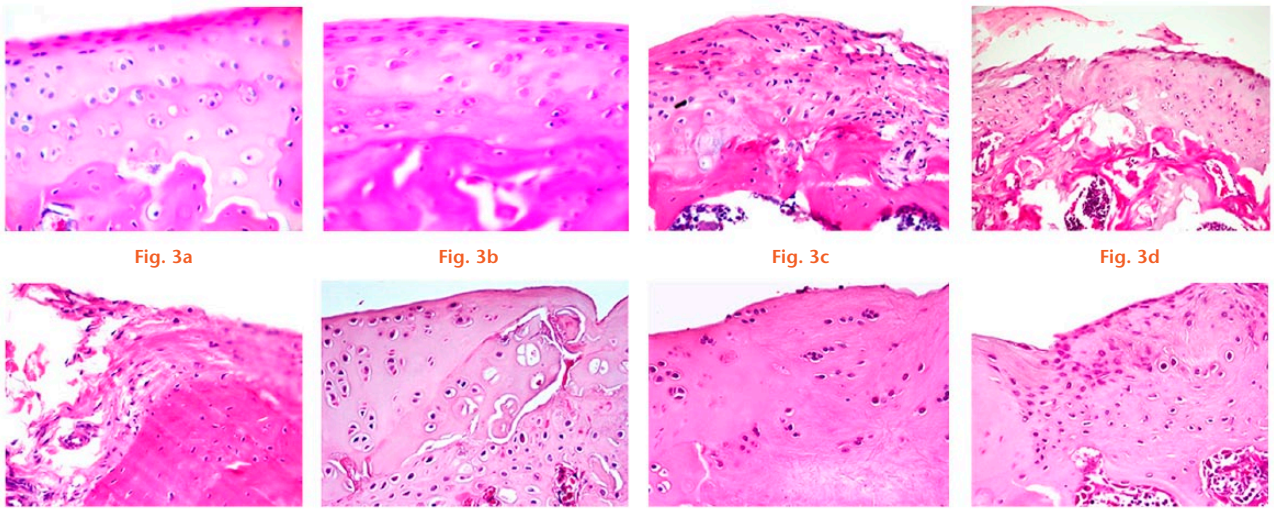

Fig. 3a Fig. 3b Fig. 3c Fig. 3d

Fig. 3e Fig. 3f Fig. 3g Fig. 3h

Histopathological evaluation of representative haematoxylin and eosin (H&E) staining sections of articular cartilage from the rat femoral condyle in the (a) naïve and (b) sham groups at 12 weeks post-surgery, and in the (c to e) anterior cruciate ligament transection (ACLT) and (f to h) osteochondral injury groups at four, eight and 12 weeks post-surgery, respectively (original magnification, x 100).

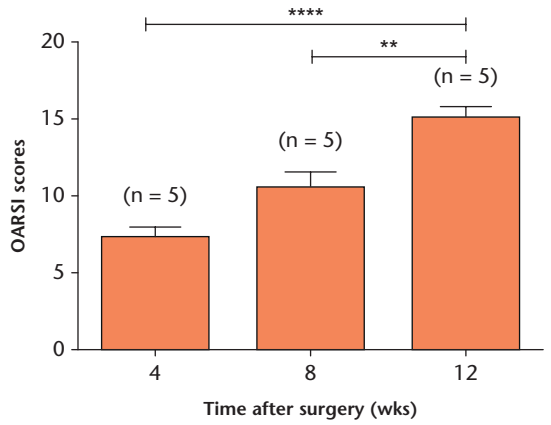

Fig. 4a

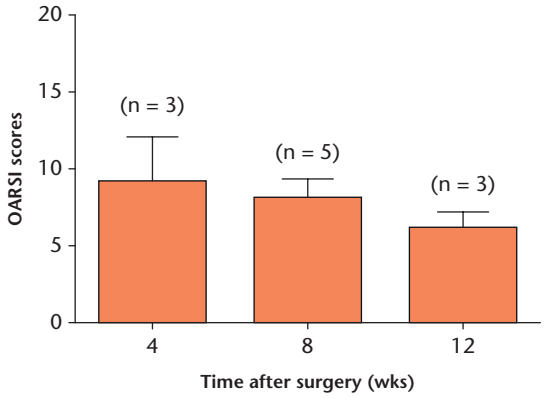

Fig. 4b

Graphs showing Osteoarthritis Research Society International (OARSI) scores obtained from the anterior cruciate ligament transection (ACLT) (a) and osteochondral defect (b) model groups at different study timepoints, including at four, eight and 12 weeks post-surgery. Values were expressed as the mean and standard error of the mean (** $p < 0.01$ and **** $p < 0.0001$).

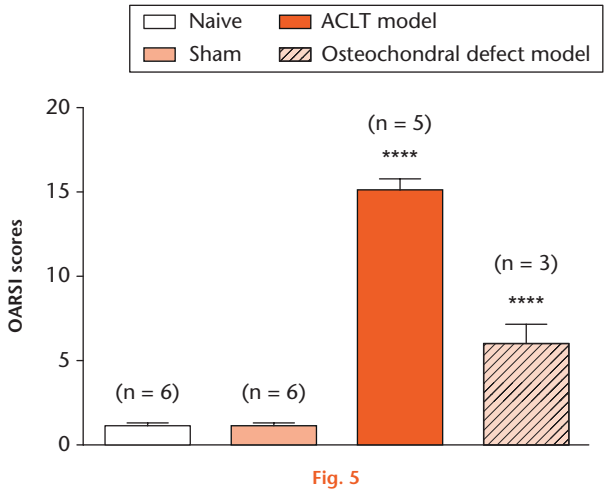

Fig. 5

Graph showing Osteoarthritis Research Society International (OARSI) scores obtained from the anterior cruciate ligament transection (ACLT) and osteochondral defect model groups at the end of the follow-up period. Values were expressed as the mean and standard error of the mean (**** $p < 0.0001$).

in the articular cartilage surfaces was found and these changes included surface irregularity and disorientation chondrocytes (Fig. 3f), erosion of a superficial layer with hypocellularity chondrocytes (Fig. 3g), and reparative tissue with fibrocartilage formation (Fig. 3h) at four, eight and 12 weeks post-surgery, respectively.

These changes were further evaluated by using the OARSI histopathology score. The mean (SEM) OARSI scores for the ACLT group, which were observed at four, eight and 12 weeks post-surgery, were 7.2 (SEM 0.7) (n = 5), 10.5 (SEM 1.0) (n = 5) and 15.2 (SEM 0.6) (n = 5), respectively (Fig. 4a). A significant difference ($p < 0.05$) in the OARSI score was also observed at 12 weeks compared with scores observed at four and eight weeks post-surgery. In contrast to the ACLT group, no significant difference in the mean (SEM) OARSI scores was observed in the osteochondral defect group at any time period, which suggests that the osteochondral defect did not contribute to the progression of OA in this model. In addition, the results from histological grading also revealed that the OA area in the ACLT animals were between stage 3 (25% to 50% involvement) and stage 4 (> 50% involvement), while in the osteochondral injury animals, the OA areas found were only between 10% and 25% involvement (stages 2 and 3).

The severity of OA progression in both models was evaluated, and the OARSI scores of both models were compared at the end of the follow-up period (12 weeks post-surgery). There was a significant difference ($p < 0.05$) in the mean (SEM) OARSI scores between both models and the sham and naïve groups. In addition, the mean (SEM) OARSI score of the ACLT model was significantly higher than that of the osteochondral injury model (15.2, SEM 0.6; 6.0, SEM 1.2) (Fig. 5).

Discussion

In this study, the development of OA-related pain behaviour patterns and the histopathological progression of OA were determined and compared between ACLT and osteochondral injury models. Pain-related behaviour was observed in both surgical groups, but the pain patterns were different. In the osteochondral injury model, pain had subsided by week 3 after surgery, whereas in the ACLT model, pain persisted throughout the study period. Consistent with this finding, the OARSI score of the ACLT model increased over a 12-week period, and was significantly higher than the osteochondral injury model score at week 12 after the operation, which suggests that the ACLT model can induce the development of OA pain in parallel with the progression of OA. The findings demonstrated that joint pain and the subsequent structural changes occur in the rat ACLT model, which is similar to previously reported results.[14,15] The finding in the ACLT animal model of progressive degenerative changes over

time with persistent pain induced behaviour might provide a good experimental model to better understand the natural history of the ACL deficient knee in humans.

A number of animal models have been described to produce OA in animal joints and these have been developed to mimic different aspects of OA. There is no single model that can reproduce all the different causes of OA. It is reported that the risk of post-traumatic OA ranges from approximately 20%, to more than 50%.[26] Understanding the natural history of post-traumatic pain may help to improve treatment of patients with joint injuries, and prevent further development of OA. Joint instability can result in pain and dysfunction and ultimately the development of OA.[27] Injury to the ACL is common, particularly in the young adult population.[28] In a long-term cohort study, it was reported that patients who sustained an ACL injury were at a substantially increased risk for the development of secondary OA in both patellofemoral and tibiofemoral joints.[29,30] Although ACL reconstruction can reduce symptoms of knee instability, a 14-year follow-up study of a randomized controlled trial, which included patients who underwent ACL reconstruction, showed a three-fold increase in OA compared with the contralateral healthy knee.[31]

Articular cartilage injury or trauma has been reported in 36% of athletes, and that incidence is more than two times higher than the general population.[32] Cartilage damage may be due to a direct traumatic injury, or associated with a repetitive injury of the joint, and it is likely to progress to OA over time. A 14-year clinical and radiological follow-up study in 28 young athletes who had isolated severe chondral damage in the weight-bearing condyles demonstrated a significant decline in athletic activity with radiological evidence of OA.[33] A number of techniques have been described to induce a reparative process for cartilage defects to restore the normal structure of cartilage in order to eliminate pain, improve function, and delay the progression of OA. In this study, the cartilage defect was produced using a K-wire inserted into the medial femoral condyle until it reached the bone marrow. The osteochondral injury is classified as international cartilage repair society (ICRS) grade 4, which is the most severe type of cartilage defect, and should represent the highest grade of cartilage injury.[34] However, the results of the histological scoring of OA did not increase over a 12-week period, which suggests there was no progression of the localized osteochodral defect to OA. This failure to progress may be as a result of the relatively short timescale between injury and histological analysis. Clinically, after an osteochondral injury pain may subside without intervention,[35] but progression in deterioration of the cartilage and the development of secondary OA progression will only be observed with long-term follow-up studies.

Pain is a common clinical feature of joint injury and can be observed in both animals and humans. The evaluation and quantification of pain in animals may be useful and relevant for clinical situations. There are several behavioural tests that can be used to assess OA pain in rodent models.[36-38] Weight-bearing asymmetry of the limb has been used as an surrogate indicator of static joint pain.[39] and will result in a robust and reproducible measure.[40,41] In this study, the pain-related behaviour was assessed by measuring changes in the mean percentage of weight-bearing distribution on the operated rat hind limb. It was observed that in both the ACLT and osteochondral injury models, there was pain related behaviour one week after surgery, but this pain only persisted in the ACLT model, for the entire study period. The pain may be caused by either knee instability or progression of the OA, or both pathologies. In contrast, the pain related behaviour disappeared by three weeks post-surgery in the osteochondral injury model. The initial pain possibly occurred from the injury and the surgery and it is likely that with healing of the surgical wound and the chondral defect, pain subsided. However, OA did not develop in the osteochondral injury as early as in the ACLT model. From this finding, we conclude that the OA-related pain behaviour induced by different types of injuries were different, and that the progression rate of OA also depends on the type of surgical model used.

The two animal models that we have studied are often used to reproduce a common orthopaedic condition in humans. Although this study in rats has shown a relationship between the pain-related behaviour and the progression of OA in both the ACLT and osteochondral injury models, there are some limitations: a small animal model may not directly reflect the clinical findings in humans, and while a larger animal model may be more clinically relevant, due to ethical concerns and the timescale required for OA to develop, studies in small animals are more appropriate for proof of concept. A further limitation in the osteochondral injury model is the standardized 1.4 mm focal defect created using K-wire. The type of injury produced in an animal model should be consistent to produce a standard change in the knee and obtain reproducible results in a preclinical study. Clinically, the osteochondral defects in the human knee will of course vary in size and degree of severity. The osteochondral defect model we have used may not be considered the standard for OA. However, this study was designed to determine the pain behaviour and the progression of OA caused by different types of injury, and to compare with the ACLT model, which is more commonly used for OA. Although we did not find OA progression in the osteochondral injury model, this may be due to the relatively short follow-up period, and further investigation over a longer study period may be required. The primary aim of this study was focused on the severity of cartilage degradation, we did not evaluate the degree of the associated synovitis. Further studies examining the synovitic changes may also help better to understand the relationship between synovitis, pain and OA progression. In addition,

the relevant underlying molecular mechanism of OA could be further investigated from this model.[42] The pain of OA is multifactorial and includes both peripheral and central nervous system components. The present study only assessed the peripheral pain by measuring the ability of the animal to bear weight on an affected limb, and although the other causes of pain in OA will not be assessed, we believe that this approach is acceptable and has been reported to produce rapid, robust and reproducible measurements in rat OA models.[9,13,43] The pain response to injury observed in both animals[44] and humans[45] varies with age, and so the experimental findings of the model that uses young animals may not be applicable to older ones. In addition, OA progression after injury also varies with age, and so it is important to compare the findings with other studies that use animals in a similar age range.

In conclusion, this study demonstrated that the pain patterns in the ACLT and osteochondral injury models are different. In addition, after histological analysis, we noted that the ACLT model produced significant OA changes, in contrast the osteochondral injury model resulted in minimal OA changes. These findings may reflect the variation in clinical findings after a knee injury, and so the selection of an appropriate model for OA in preclinical studies should be specific and relevant to the clinical scenario.

References

1. **Hinton R, Moody RL, Davis AW, Thomas SF.** Osteoarthritis: diagnosis and therapeutic considerations. *Am Fam Physician* 2002;65:841-848.
2. **Sarzi-Puttini P, Cimmino MA, Scarpa R, et al.** Osteoarthritis: an overview of the disease and its treatment strategies. *Semin Arthritis Rheum* 2005;35(Suppl 1):1-10.
3. **Wysocka-Skurska I, Sierakowska M, Kułak W.** Evaluation of quality of life in chronic, progressing rheumatic diseases based on the example of osteoarthritis and rheumatoid arthritis. *Clin Interv Aging* 2016;11:1741-1750.
4. **Amin AK, Simpson AHRW, Hall AC.** Iatrogenic articular cartilage injury: the elephant in the operating theatre. The surgeons' role in chondroprotection. *Bone Joint J* 2017;99-B:1555-1556.
5. **Ross M, Wiemann M, Peters SE, Benson R, Couzens GB.** The influence of cartilage thickness at the sigmoid notch on inclination at the distal radioulnar joint. *Bone Joint J* 2017;99-B:369-375.
6. **Little CB, Smith MM.** Animal models of osteoarthritis. *Curr Rheumatol Rev* 2008;4:1-8.
7. **Pelletier J-P, Boileau C, Altman RD, Martel-Pelletier J.** Animal models of osteoarthritis. In: Hochberg MC, Silman AJ, Smolen JS, Weinblatt ME, Weisman MH, eds. *Rheumatology*. Philadelphia: Mosby/Elsevier, 2011:1731-1739.
8. **Pritzker KP.** Animal models for osteoarthritis: processes, problems and prospects. *Ann Rheum Dis* 1994;53:406-420.
9. **Bove SE, Calcaterra SL, Brooker RM, et al.** Weight bearing as a measure of disease progression and efficacy of anti-inflammatory compounds in a model of monosodium iodoacetate-induced osteoarthritis. *Osteoarthritis Cartilage* 2003;11:821-830.
10. **Bendele AM.** Animal models of osteoarthritis. *J Musculoskelet Neuronal Interact* 2001;1:363-376.
11. **Ameye LG, Young MF.** Animal models of osteoarthritis: lessons learned while seeking the "Holy Grail". *Curr Opin Rheumatol* 2006;18:537-547.
12. **Zlotnicki JP, Naendrup JH, Ferrer GA, Debski RE.** Basic biomechanic principles of knee instability. *Curr Rev Musculoskelet Med* 2016;9:114-122.
13. **Pomonis JD, Boulet JM, Gottshall SL, et al.** Development and pharmacological characterization of a rat model of osteoarthritis pain. *Pain* 2005;114:339-346.
14. **Hayami T, Pickarski M, Zhuo Y, et al.** Characterization of articular cartilage and subchondral bone changes in the rat anterior cruciate ligament transection and meniscectomized models of osteoarthritis. *Bone* 2006;38:234-243.
15. **Naito K, Watari T, Furuhata A, et al.** Evaluation of the effect of glucosamine on an experimental rat osteoarthritis model. *Life Sci* 2010;86:538-543.
16. **Garstang SV, Stitik TP.** Osteoarthritis: epidemiology, risk factors, and pathophysiology. *Am J Phys Med Rehabil* 2006;85(11 Suppl):S2-S11.
17. **Niemeyer P, Feucht MJ, Fritz J, et al.** Cartilage repair surgery for full-thickness defects of the knee in Germany: indications and epidemiological data from the German Cartilage Registry (KnorpelRegister DGOU). *Arch Orthop Trauma Surg* 2016;136:891-897.
18. **Chu CR, Szczodry M, Bruno S.** Animal models for cartilage regeneration and repair. *Tissue Eng Part B Rev* 2010;16:105-115.
19. **Bhosale AM, Richardson JB.** Articular cartilage: structure, injuries and review of management. *Br Med Bull* 2008;87:77-95.
20. **Kuyinu EL, Narayanan G, Nair LS, Laurencin CT.** Animal models of osteoarthritis: classification, update, and measurement of outcomes. *J Orthop Surg* 2016;11:19.
21. **Kazemi D, Shams Asenjan K, Dehdilani N, Parsa H.** Canine articular cartilage regeneration using mesenchymal stem cells seeded on platelet rich fibrin: Macroscopic and histological assessments. *Bone Joint Res* 2017;6:98-107.
22. **Khunakornvichaya A, Lekmeechai S, Pham PP, et al.** Morus alba L. stem extract attenuates pain and articular cartilage damage in the anterior cruciate ligament transection-induced rat model of osteoarthritis. *Pharmacology* 2016;98:209-216.
23. **Castro RR, Cunha FQ, Silva FS Jr, Rocha FA.** A quantitative approach to measure joint pain in experimental osteoarthritis-evidence of a role for nitric oxide. *Osteoarthritis Cartilage* 2006;14:769-776.
24. **Dausse Y, Grossin L, Miralles G, et al.** Cartilage repair using new polysaccharidic biomaterials: macroscopic, histological and biochemical approaches in a rat model of cartilage defect. *Osteoarthritis Cartilage* 2003;11:16-28.
25. **Pritzker KP, Gay S, Jimenez SA, et al.** Osteoarthritis cartilage histopathology: grading and staging. *Osteoarthritis Cartilage* 2006;14:13-29.
26. **Brown TD, Johnston RC, Saltzman CL, Marsh JL, Buckwalter JA.** Posttraumatic osteoarthritis: a first estimate of incidence, prevalence, and burden of disease. *J Orthop Trauma* 2006;20:739-744.
27. **Kuršumović K, Charalambous CP.** Graft salvage following infected anterior cruciate ligament reconstruction: a systematic review and meta-analysis. *Bone Joint J* 2016;98-B:608-615.
28. **Longo UG, Ciuffreda M, Casciaro C, et al.** Anterior cruciate ligament reconstruction in skeletally immature patients: a systematic review. *Bone Joint J* 2017;99-B:1053-1060.
29. **Ahmed I, Salmon L, Roe J, Pinczewski L.** The long-term clinical and radiological outcomes in patients who suffer recurrent injuries to the anterior cruciate ligament after reconstruction. *Bone Joint J* 2017;99-B:337-343.
30. **Neuman P, Englund M, Kostogiannis I, et al.** Prevalence of tibiofemoral osteoarthritis 15 years after nonoperative treatment of anterior cruciate ligament injury: a prospective cohort study. *Am J Sports Med* 2008;36:1717-1725.
31. **Barenius B, Ponzer S, Shalabi A, et al.** Increased risk of osteoarthritis after anterior cruciate ligament reconstruction: a 14-year follow-up study of a randomized controlled trial. *Am J Sports Med* 2014;42:1049-1057.
32. **Flanigan DC, Harris JD, Trinh TQ, Siston RA, Brophy RH.** Prevalence of chondral defects in athletes' knees: a systematic review. *Med Sci Sports Exerc* 2010;42:1795-1801.
33. **Messner K, Maletius W.** The long-term prognosis for severe damage to weight-bearing cartilage in the knee: a 14-year clinical and radiographic follow-up in 28 young athletes. *Acta Orthop Scand* 1996;67:165-168.
34. **Dwyer T, Martin CR, Kendra R, et al.** Reliability and validity of the arthroscopic international cartilage repair society classification system: correlation with histological assessment of depth. *Arthroscopy* 2017;33:1219-1224.
35. **van Dijk CN, Reilingh ML, Zengerink M, van Bergen CJ.** Osteochondral defects in the ankle: why painful? *Knee Surg Sports Traumatol Arthrosc* 2010;18:570-580.
36. **Yu YC, Koo ST, Kim CH, et al.** Two variables that can be used as pain indices in experimental animal models of arthritis. *J Neurosci Methods* 2002;115:107-113.
37. **Min SS, Han JS, Kim YI, et al.** A novel method for convenient assessment of arthritic pain in voluntarily walking rats. *Neurosci Lett* 2001;308:95-98.
38. **Malfait AM, Little CB, McDougall JJ.** A commentary on modelling osteoarthritis pain in small animals. *Osteoarthritis Cartilage* 2013;21:1316-1326.
39. **Christiansen CL, Stevens-Lapsley JE.** Weight-bearing asymmetry in relation to measures of impairment and functional mobility for people with knee osteoarthritis. *Arch Phys Med Rehabil* 2010;91:1524-1528.
40. **Andruski B, McCafferty DM, Ignacy T, Millen B, McDougall JJ.** Leukocyte trafficking and pain behavioral responses to a hydrogen sulfide donor in acute monoarthritis. *Am J Physiol Regul Integr Comp Physiol* 2008;295:R814-R820.
41. **Suokas AK, Walsh DA, McWilliams DF, et al.** Quantitative sensory testing in painful osteoarthritis: a systematic review and meta-analysis. *Osteoarthritis Cartilage* 2012;20:1075-1085.

42. **Yin C-M, Suen W-C-W, Lin S, et al.** Dysregulation of both miR-140-3p and miR-140-5p in synovial fluid correlate with osteoarthritis severity. *Bone Joint Res* 2017;6:612-618.
43. **Wen ZH, Tang CC, Chang YC, et al.** Glucosamine sulfate reduces experimental osteoarthritis and nociception in rats: association with changes of mitogen-activated protein kinase in chondrocytes. *Osteoarthritis Cartilage* 2010;18:1192-1202.
44. **Yezierski RP.** The effects of age on pain sensitivity: preclinical studies. *Pain Med* 2012;13(Suppl 2):S27-S36.
45. **Riley JL III, Cruz-Almeida Y, Glover TL, et al.** Age and race effects on pain sensitivity and modulation among middle-aged and older adults. *J Pain* 2014;15:272-282.

Acknowledgements

- The authors would like to thank Professor S. Hongeng and Ramathibodi Research Centre for academic support.

Funding Statement

- O. Sriwatananukulkit was supported by the Science Achievement Scholarship of Thailand. This work was also supported by a collaborative research project grant (#SC-RA2559-3) from the Faculty of Science and the Faculty of Medicine at Ramathibodi Hospital, Mahidol University and the Thailand Research Fund (MRG5980107).

Author Contribution:

- T. Tawonsawatruk: Designed the experiments, Analyzed and interpreted the data, Drafted and revised the manuscript.
- O. Sriwatananukulkit: Designed the experiments, Performed the experiments.
- W. Himakhun: Participated in histological scoring, Interpretation of the histological results.
- W. Hemstapat: Designed the experiments, Analyzed and interpreted the data, Drafted, revised and approved the final submitted manuscript.

Conflicts of Interest Statement

- None declared.